ACTIVE VIBRATION CONTROL OF COMPLEX STRUCTURES IN MODAL SPACE

A THESIS SUBMITTED TO
THE GRADUATE SCHOOL OF NATURAL   AND APPLIED SCIENCES
OF
MIDDLE EAST TECHNICAL UNIVERSITY

BY
KEMAL MERSİN

IN PARTIAL FULFILLMENT OF THE

REQUIREMENTS
FOR
THE DEGREE OF MASTER OF SCIENCE
IN
MECHANICAL ENGINEERING

DECEMBER 2014

Approval of the thesis:

ACTIVE VIBRATION CONTROL OF COMPLEX STRUCTURES IN MODAL SPACE

submitted by **KEMAL MERSİN** in partial fulfillment of the requirements for the degree of **Master of Science in Mechanical Engineering Department, Middle East Technical University** by,

Prof. Dr. Gülbin Dural Ünver
Dean, Graduate School of **Natural and Applied Sciences**   _____

Prof. Dr. R. Tuna Balkan
Head of Department, **Mechanical Engineering**   _____

Assist. Prof. Dr. Yiğit Yazıcıoğlu
Supervisor, **Mechanical Engineering Dept., METU**   _____

Assoc. Prof. Dr. Melin Şahin
Co-Supervisor, **Aerospace Engineering Dept., METU**   _____

Examining Committee Members:

Prof. Dr. Mehmet Çalışkan
Mechanical Engineering Dept., METU   _____

Assist. Prof. Dr. Yiğit Yazıcıoğlu
Mechanical Engineering Dept., METU   _____

Assoc. Prof. Dr. Melik Dölen
Mechanical Engineering Dept., METU   _____

Assoc. Prof. Dr. Ender Ciğeroğlu
Mechanical Engineering Dept., METU   _____

Assist. Prof. Dr. A. Türker Kutay
Aerospace Engineering Dept., METU   _____

                                        Date: 03.12.2014

I hereby declare that all information in this document has been obtained and presented in accordance with academic rules and ethical conduct. I also declare that, as required by these rules and conduct, I have full cited and referenced all material and results that are not original to this work.

Name, Last Name: Kemal Mersin

Signature:

ABSTRACT

ACTIVE VIBRATION CONTROL OF COMPLEX STRUCTURES IN MODAL SPACE

Mersin, Kemal
M.S., Department of Mechanical Engineering
Supervisor: Assist. Prof. Dr. Yiğit Yazıcıoğlu
Co-Supervisor: Assoc. Prof. Dr. Melin Şahin

December 2014, 89 pages

Aerospace structures are designed to be light-weight to obtain high performance. Reduction in weight makes the structure flexible and lower frequency modes can be easily excited. Moreover those modes have low damping and vibrations do not attenuate immediately. Passive systems are effective to control the vibrations but they can be heavy and most of the time they do not respond to changing environment conditions. An active system is necessary for low-weight adaptive vibration reduction system.

Modal Space Control is used for large flexible aerospace structures due to the advantage of reducing the complexity of control system. In this study a generalized formulation of modal space control is proposed for three dimensions where each node is modeled with six degrees of freedom.

Keywords: Active vibration control, state space control, modal control, finite element analysis.

ÖZ

MODAL UZAYDA KARMAŞIK YAPILARIN AKTİF TİTREŞİM KONTROLÜ

Mersin, Kemal
Yüksek Lisans, Makina Mühendisliği Bölümü
Tez Yöneticisi:　　　Yrd.Doç.Dr. Yiğit Yazıcıoğlu
Ortak Tez Yöneticisi: Doç.Dr. Melin Şahin

Aralık 2014, 89 sayfa

Yüksek performans elde etmek için havacılık ve uzay yapıları hafif olarak tasarlanmaktadır. Ağırlığın azaltılması yapıyı daha esnek hale getirmekte ve düşük frekanstaki modlar kolaylıkla tahrik edilebilmektedirler. Ayrıca bu modlardaki sönümleme oranı düşüktür ve titreşimler hemen kaybolmamaktadır. Pasif sistemler titreşimin sönümlenmesinde etkili olsalarda, ağır olabilirler ve değişen çevre şartlarına çoğu zaman uyum sağlayamazlar. Hafif ve çevre şartlarına uyum sağlayabilen titreşim azaltma sistemi için aktif titreşim kontrolü gereklidir.

Kontrol sisteminin karmaşıklığını azaltması sebebiyle büyük ve esnek havacılık ve uzay yapılarında Modal Uzay Kontrolü kullanılmaktadır. Bu çalışmada her noktanın altı serbestlik derecesi ile modellendiği üç boyutlu yapılar için modal uzay kontrolünün genel formülasyon önerilmiştir.

Anahtar Kelimeler: Aktif titreşim kontrolü, durum uzay kontrolü, modal control, sonlu elemanlar analizi.

To My Family

ACKNOWLEDGMENTS

TABLE OF CONTENTS

LIST OF TABLES

TABLES

LIST OF FIGURES

ABBREVIATIONS

SDOF : Single Degree of Freedom

FEA : Finite Element Analysis

FEM : Finite Element Method

IMSC : Independent Modal Space Control

N : Number of nodes

m : Number of modes

mc : Number of controlled modes

mr : Number of residual modes

d : Number of degrees of freedom

DOF : Degrees of Freedom

η : Modal displacement

ϕ : Mode shape vector

Φ : Mode shape matrix

I : Identity matrix

Ω : Natural frequency in rad/sec

ζ : Modal damping ratio

CHAPTER 1

INTRODUCTION

1.1   General Introduction

Rigidity and weight are often competing objectives for high performance structures such as the ones in aerospace applications. In these structures, first natural frequencies and damping ratios at those frequencies are usually quite low. Therefore, they are prone to high vibration levels during normal operation. Excessive vibration may cause the following problems in these applications:

- Disturbs the crew through vibration and noise
- Decreases service life
- Damages electronic components
- Damages the structure
- Reduces the accuracy of precise structures

Helicopter applications can be taken as an example for such high performance structures where rotor is the main vibration source. N/rev frequency vibration in the helicopter is dominant excitation. For the constant rotor speed helicopter's passive vibration isolation systems are effective in forward flight / hover conditions. Those systems are heavy and ineffective at maneuvering flight and requires continuous maintenance. Their performance degrade due to the changing properties of system. Furthermore they are not adaptive for rotor rotation speed changes. Active systems can overcome the weight problem, and they can adapt to changing conditions. [1, 2]. The current trend in helicopter vibration control is given in Figure 1-1 where weight reduction with increased efficiency is required.
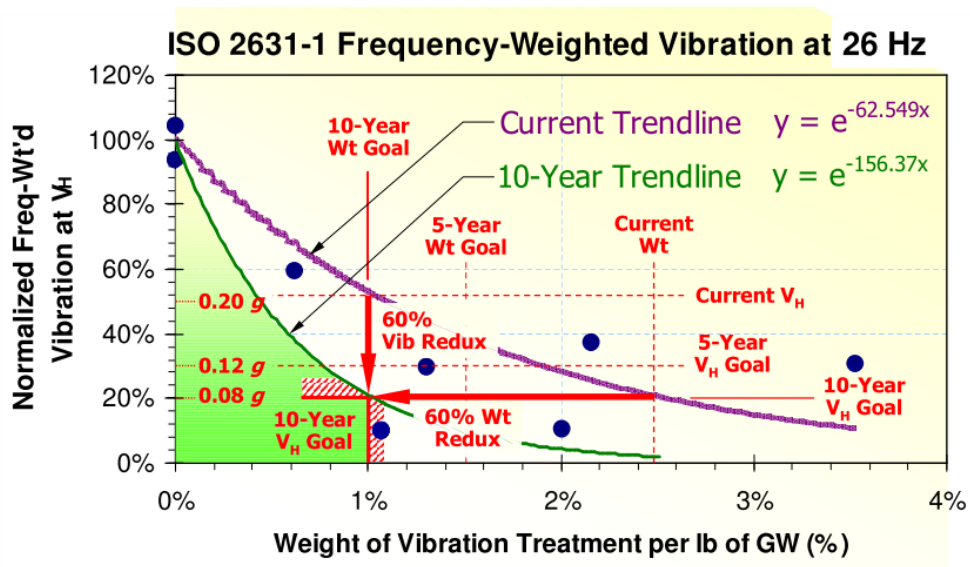
Figure 1-1 – Helicopter AVC Trend [1]

Satellites are another type of high performance lightweight and underdamped structures that can be excited due to the maneuvers in space. Solar panels and antennas can oscillate for extended periods with those excitations. This type of vibrations reduce the accuracy of the sensors such as telescopes or synthetic aperture radars. [3, 4, 5], Vibrations also degrade the performance of cameras on board [6]. An image of international space station is presented in Figure 1-2 to show the solar panels. Each panel length is 33 meters and width is 4.6 meters. Their first two modes are 0.6 and 0.8 Hz. In addition to operational vibrations in space, satellites are affected by high vibrations during launch due to the combustion instability [7, 8] which produce longitudinal vibrations. For example Apollo 13 was subject to 34g vibration level at 16 Hz.

Figure 1-2 – International Space Station

1.2 Literature Review

Controlling vibrations of large flexible structures in physical domain is a high degree of freedom problem. Meirovitch and Balas proposed a new control algorithm called modal space control, where vibrations are controlled in modal domain [9, 10]. Therefore degrees of freedom of the system model reduce to the number of modelled modes.

Optimal control strategies such as Linear Quadratic Regulator (LQR) and Linear Quadratic Gaussian (LQG) has been studied for modal space control. . Optimal control is also applied to damped gyroscopic systems [11, 12, 13].

Modal space control is first designed for distributed systems. It is expanded to discrete systems for point acted sensors and actuators. Modal filters and interpolation functions are used for this expansion [14].

In the distributed system, considering infinity modes, there are no observer or control spillover problems. However in reality it is necessary to truncate modelled modes where observation spillover can be a problem. By increasing number of modelled modes, observation spillover can be solved [15].

Active vibration control is used to control low frequency vibrations. The effects of controller to higher modes create control spillover problem. However exciting higher modes requires more energy, those modes have lower amplitudes and due their random nature they cancel each other [14].

It is observed in the literature that optimal placement of sensors and actuators for modal space control is studied for plate type structures [16, 17, 18].

Integrated structural design with active vibration control has also been investigated with modal space control to optimize actuator and sensor locations while minimizing the mass of the structure [19, 20].

Modal space control is divided into two sub divisions called coupled control and Independent Modal Space Control (IMSC). In IMSC each mode is controlled separately and every modal equation is decoupled. Designing control systems for IMSC is easy and finding global minimum is possible. In coupled control less number of actuators can be used however the performance is sensitive to actuator locations and finding global minimum is not always possible [21].

Meirovitch and Baruh shown that independent modal space control close loop system is guaranteed to be stable. It is stated that any error in mass or stiffness matrices does not create any instabilities in the closed loop system where an appropriate feedback matrix is chosen [22].

In normal IMSC approach, a separate actuator is required for controlling each mode. In [16] a new formulation is proposed to optimal control law to control same number of modes with less actuators. In spite of this advantages, now the quadratic cost function does not reflect one-to-one correspondence between adjustable parameters and actuators control effort and the connection between state penalty and state performance is indirect. Therefore, tuning of the controller is more troublesome. The third problem is that in this approach stability is not assured and one must take care of stability during the adjustment of controller parameters.

Baz, Poh and Studer suggested a modified independent modal space control (MIMSC) method to overcome spillover problem in IMSC [23]. They also offered an optimal actuator placement technique, uni-variate search method which varies the location of one actuator at a time in order to minimize a cost function. It is stated that optimal controller solves the problem in modal domain, an optimal location is necessary to minimize control forces in actual domain. Thirdly, a time sharing methodology is studied where small number of actuators suppress large number of modes. Two strategies are suggested, first is sequential which every mode is given a fixed amount of time to suppress vibrations. Second method is based on modal energy where the highest energy n number of modes are suppressed with n number of actuators. The drawback of time sharing is actuators are required to have wide bandwidth.

Singh proposes an efficient modal control algorithm which improves the MIMSC algorithm. In MIMSC when energy in each mode is equal, controller chatters. With the proposed algorithm the chatter is prevented where each mode weight is proportional to its displacement or energy content. Also in this paper it is shown that one piezo-electric actuator can be used to control more than one mode [24].

In Öz's paper it is stated that the main criticism of IMSC is that it requires many actuators and sensors to be implemented in real structures [25]. Öz has made the connection between the piezoelectric patches with independent modal space control approach in his paper. It is shown that one piezoelectric patch can be used to reduce vibrations of more than one mode [24].

Fang et al. proposed a modified independent modal space control algorithm to solve spillover problem for uncontrolled modes [26]. They have suggested a new feedback algorithm where uncontrolled modeled modes spillover can be prevented as long as controller design follows the given rules in the paper. The effects of residual modes and their connection with optimal controller law is shown mathematically and nullifying them solves the spillover problem.

Silva and Inman has studied IMSC on internal variable based viscoelastic bar considering the internal variables [23]. A finite element model for longitudinal vibrations of viscoelastic elements are built. The model is one-dimensional with one degrees of freedom. IMSC is tested numerically and the reduction of vibration is satisfactory. It is stated that viscoelastic material have high damping at higher frequencies and IMSC can be used for only suppressing lower modes which makes IMSC an attractive approach to be used with viscoelastic systems.

Raja et al. studied the effects of one and two dimensional piezoelectric actuation on smart panels where IMSC is used as the controller. Directional piezoelectric and isotropic piezoelectric actuation behavior is compared numerically on aluminum plates. Plates are modeled with four-node Mindlin-Reissner plate element. The model is three dimensional containing five degrees of freedom. Mode shapes are found with finite element analysis.

In a study by Meirovitch and Oz, a flexible spacecraft is considered with 12 modes of two cantilever appendages in three dimensions shown in Figure 1-3. Assumed functions are used as mode shapes. Moreover rigid modes of the spacecraft both translation and rotation were controlled with the actuators located at the center [11].
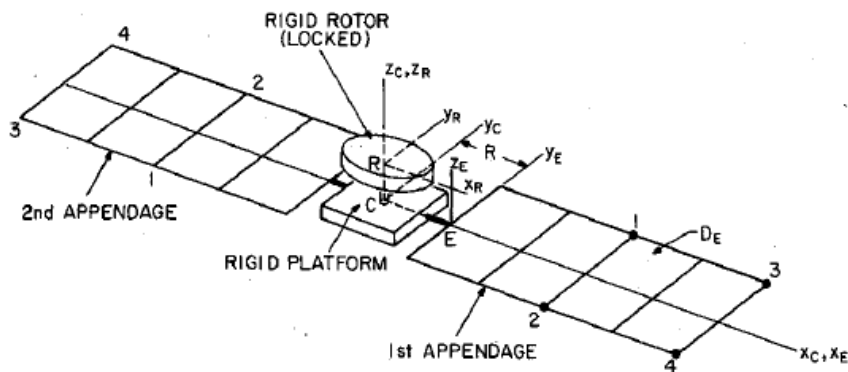
Figure 1-3 Spaceraft Model

In [27] a non-classically damped gyroscopic system is studied by Lin and Yu. Mode shapes are calculated by mode shape functions. The system is one dimensional where degrees of freedom of each node is four with two translations and two rotations. IMSC is effectively applied on the system.
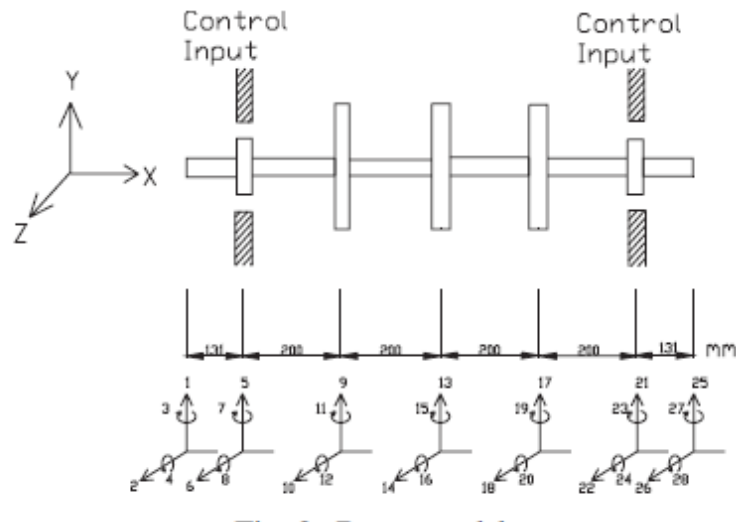
Figure 1-4 Rotor Model

Houlstan et al. presented a novel modal control method that can be applied to the non-classically damped systems. A similar model shown in Figure 1-4 is numerically tested with the new control algorithm [28].

Hurlebaus et al studied IMSC on curved panels. In the study they have found mode shapes with experimental modal analysis. They modeled the structure in three dimensions x, y, z and used three degrees of freedom in each orthogonal translation axis. An experimental modal control study is carried out and it is shown that IMSC can be applied on curved panels. Mode shapes of the curved panel is shown in Figure 1-5 [29].

Mode	Eigenfrequency f_j [Hz]	Damping ratio ζ_j [%]
1	196.56	1.10
2	281.65	1.00
3	457.02	1.45
4	500.31	1.25
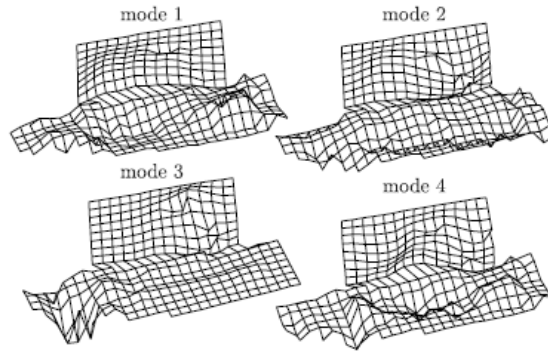
Figure 1-5 Experimental mode shapes, natural frequencies and damping ratio of curved panels of car,

Serra, Resta and Ripamonti proposed a new method called dependent modal space controller where in addition to IMSC, mode shapes can be altered to create nodes at wanted locations [30]. However to alter mode shapes more control force is required. A cantilever beam with mode shapes taken from finite element analysis is numerically tested. In Figure 1-6 the adjusted first three mode shapes of the cantilever beam are shown.
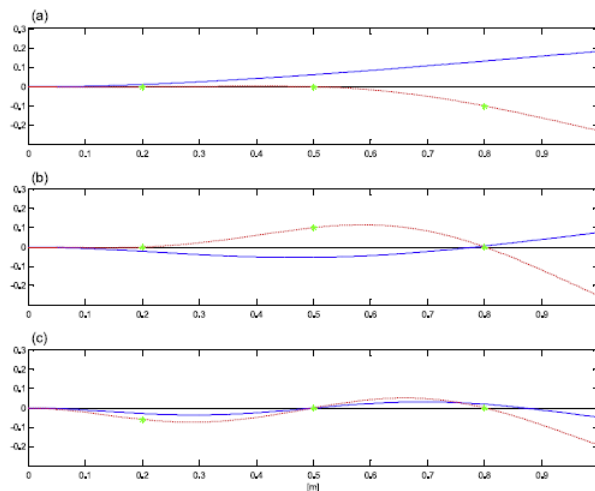
Figure 4. DMSC eigenvector assignment: original (continuous line) and imposed (dotted line) mode shapes (star markers); mode 1 at 5.27 Hz (a), mode 2 at 33.02 Hz (b), mode 3 at 92.46 Hz (c).

Figure 1-6 Adjusted Mode Shapes

8

1.3   Problem Definition

Large flexible structures have low frequency and low damping in the first modes which requires attention to prevent excessive vibration levels. Passive solutions are too heavy to be implemented on to aerospace structures. Therefore an active vibration control solution is required.

1.4   Motivation

Controlling the first modes of large flexible structures is necessary due to the points stated in the problem definition. An implementation on complex shapes is not frequently encountered in literature. In this study, implementation of modal space control approach will be extended to an arbitrary 3-D complex shape.

1.5   Objective and Scope of This Thesis

The objective of this study is to propose a generalized formulation in three dimensions and show that modal space control can be applied to complex structures. The outline of the thesis is as follows; a general introduction and literature survey is presented in Chapter 1. Modal space representation of a one dimensional structure is given in the Chapter 2. Discretization and generalization of a three dimensional structure in modal space is studied in Chapter 3. In Chapter 4 controller and observer design is shown. Case studies for simply supported beam and a three dimensional shape is presented in Chapter 5. Discussion, conclusion and future work is given in the Chapter 6.

CHAPTER 2

MODAL SPACE REPRESENTATION OF A 1D STRUCTURE

2.1   Introduction

This chapter presents the theory behind the modal space representation of a 1-D distributed structure. A structure with closed form solution is used to compare the model. Euler-Bernoulli beam is used to analytically express the bending vibrations of beams.

First a simply supported beam will be modelled with appropriate Partial Differential Equation (PDE) and it will be solved for natural frequencies and corresponding mode shapes. Second orthogonality property will be shown. With the result of orthogonality property it will be shown that the response of the beam can be written as sum of mode shapes. It is called the expansion theorem. It is known that every mode is independent of each other and they are decoupled in the modal domain by orthogonality theorem.

Then the modal space equations of the structure will be modelled in state space. To validate the state space model a simply supported beam response will be used.

2.2   Simply supported beam natural frequency and mode shapes

Euler-Bernoulli beam theory is used to model the transverse bending vibrations of a beam shown in the Figure 2.1. The governing PDE of the beam can be written as [31]

$$-\frac{\partial^2}{\partial x^2}\left[EI(x)\frac{\partial^2 y(x,t)}{\partial x^2}\right] + f(x,t) = m(x)\frac{\partial^2 y(x,t)}{\partial t^2} \qquad (2.1)$$

Where $y(x,t)$ is the transverse displacement, $f(x,t)$ is the transverse force per unit length, $m(x)$ the mass per unit length, $EI(x)$ is the flexural rigidity which E is the modulus of elasticity and $I(x)$ is the cross sectional area moment of inertia about an axis normal to x and y and passing through the center of the cross section.
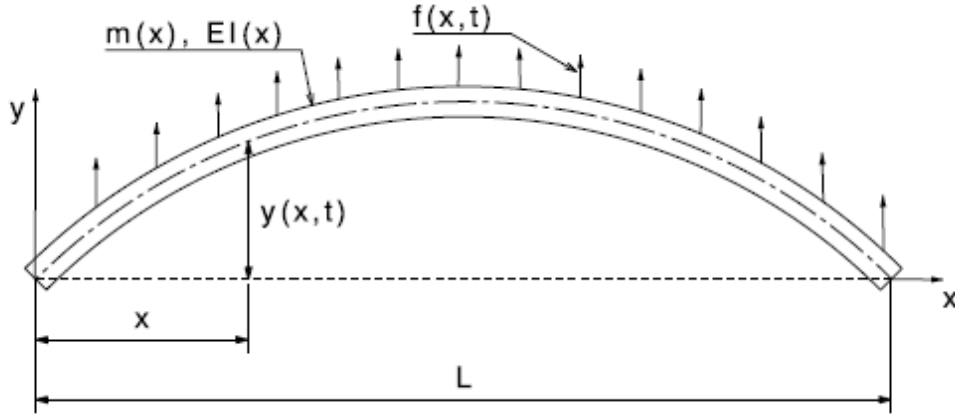
Figure 2-1 Euler Bernoulli Beam

It is known that the spatial solution is independent from the temporal solution which implies that the y and t are separable variables. Then the displacement can be expressed as

$$y(x,t) = Y(x)F(t) \tag{2.2}$$

Placing (2.2) into (2.1), neglecting the force term and dividing both sides by $F(t)$, equation (2.1) reduces to

$$\frac{d^2}{dx^2}\left[EI(x)\frac{d^2Y(x)}{dx^2}\right] = \omega^2 m(x)Y(x), 0 < x < \tag{2.3}$$

Simply supported beam is pinned from two ends. The boundary conditions for pinned end are zero displacement and zero moment at the pinned point. It can be written as

$$Y(x) = 0, \qquad M(x,t) = EI(x)\frac{d^2Y(x)}{dx^2} = 0 \tag{2.4}$$

For demonstration a beam with constant cross section area and material properties with length L will be used. No external force is given. Then the equation (2.1) reduces to

$$\frac{d^4Y(x)}{dx^4} - \beta^4 y = 0, 0 < x < L;, \beta^4 = \frac{\omega^2 m}{EI} \tag{2.5}$$

And boundary conditions are

12

$$Y(x) = 0, \frac{d^2Y(x)}{dx^2} = 0, x = 0, L \qquad (2.6)$$

Assume a solution for equation (2.5) as

$$Y(x) = Asin\beta x + Bcos\beta x + Csinh\beta x + Dcosh\beta x \qquad (2.7)$$

The A, B, C, D constants will be evaluated from the boundary conditions. Only three constants can be found and the fourth will be written to derive the characteristic equation for β. From the boundary conditions,

$$\frac{d^2Y(x)}{dx^2} = \beta^2[-Asin\beta x - Bcos\beta x + Csinh\beta x + Dcosh\beta x] \qquad (2.8)$$

At x = 0 it can be written that

$$Y(0) = B + D = 0 \qquad (2.9)$$

And

$$\frac{d^2Y(x)}{dx^2}\bigg|_{x=0} = -B + D = 0 \qquad (2.10)$$

Which implies that $B = D = 0$. At $x = L$ it can be written that

$$Y(L) = Asin\beta L + Csinh\beta L = 0 \qquad (2.11)$$

And

$$\frac{d^2Y(x)}{dx^2}\bigg|_{x=L} = \beta^2(-Asin\beta L + Csinh\beta L) = 0 \qquad (2.12)$$

$\beta = 0$ is a trivial solution so it is not a solution. It implies that $C = 0$ and

$$sin\beta L = 0 \qquad (2.13)$$

(2.13) is the characteristic equation for simply supported beam. The solution of this equation consists of infinite number of eigenvalues

$$B_r L = r\pi, \qquad r = 1,2, \dots \qquad (2.14)$$

Then the eigenfunctions can be written by equating B, C, D to 0 and re-writing the equation (2.7) with (2.14);

$$Y_r(x) = A_r sin\beta_r x = A_r sin\frac{r\pi x}{L}, \qquad r = 1,2,\dots \qquad (2.15)$$

The natural frequencies of the system can be found from

$$\beta^4 = \frac{\omega^2 m}{EI} \qquad (2.16)$$

Then using equation (2.14) and rewriting (2.16) will yield

$$\omega_r = r^2\pi^2\sqrt{\frac{EI}{mL^4}}, \qquad r = 1,2,\dots \qquad (2.17)$$

First three modes of simply supported beam are drawn below in Figure 2-2.
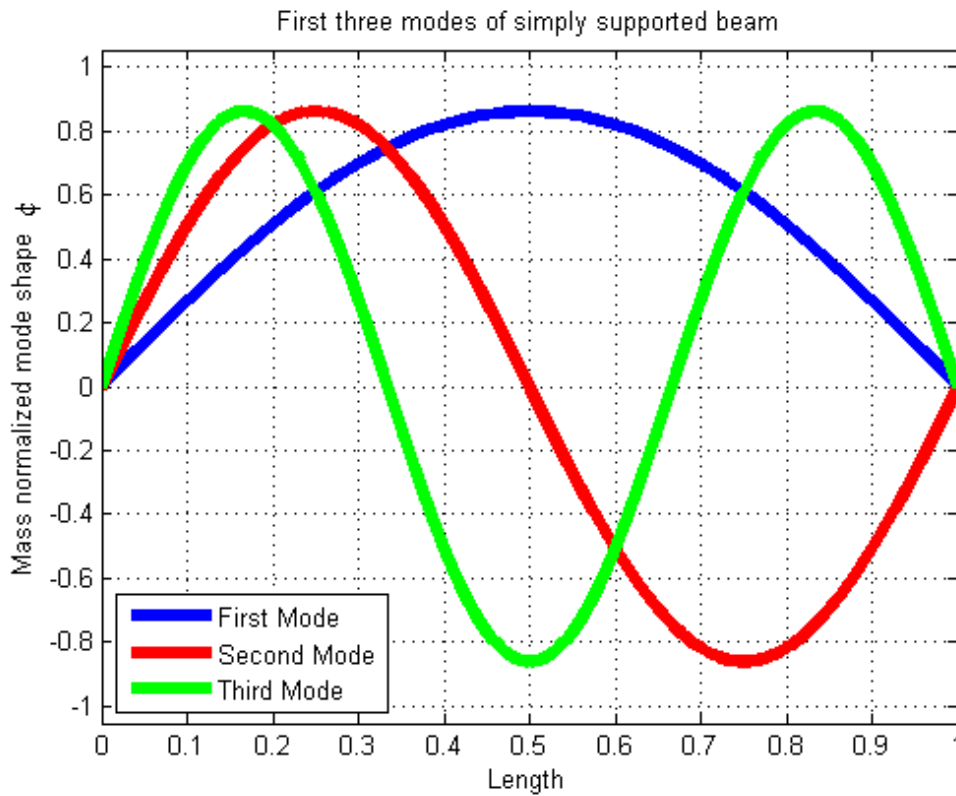
Figure 2-2 First three modes of simply supported beam

2.3 Orthogonality of Modes and Expansion Theorem

Consider two distinct solutions for equation (2.15) and (2.17) as $Y_r(x), \omega_r^2$ and $Y_s(x), \omega_s^2$ and write the governing beam equation

$$\frac{d^2}{dx^2}\left[EI(x)\frac{d^2Y_r(x)}{dx^2}\right] = \omega_r^2 m(x)Y_r(x), \quad 0 < x < L \tag{2.18}$$

And

$$\frac{d^2}{dx^2}\left[EI(x)\frac{d^2Y_s(x)}{dx^2}\right] = \omega_s^2 m(x)Y_s(x), \quad 0 < x < L \tag{2.19}$$

Then multiply (2.18) with $Y_s(x)$ and integrate over L. Then rewrite it,

$$\int_0^L Y_s(x)\frac{d^2}{dx^2}\left[EI(x)\frac{d^2Y_r(x)}{dx^2}\right]dx = \omega_r^2\int_0^L m(x)Y_s(x)Y_r(x)\,dx \tag{2.20}$$

Integrating by parts the left side twice we obtain the following equation

$$\int_0^L Y_s(x)\frac{d^2}{dx^2}\left[EI(x)\frac{d^2Y_r(x)}{dx^2}\right]dx$$
$$= Y_s(x)\frac{d}{dx}\left[EI(x)\frac{d^2Y_r(x)}{dx^2}\right]_0^L$$
$$- \left[\frac{dY_s(x)}{dx}EI(x)\frac{d^2Y_r(x)}{dx^2}\right]_0^L$$
$$+ \int_0^L EI(x)\frac{d^2Y_r(x)}{dx^2}\frac{d^2Y_s(x)}{dx^2} \tag{2.21}$$

For pinned case, the boundary conditions from (2.6) imply that

$$\frac{d^2Y(x)}{dx^2} = 0, x = 0, L$$

Then (2.21) is reduced to

$$\int_0^L EI(x)\frac{d^2Y_r(x)}{dx^2}\frac{d^2Y_s(x)}{dx^2} \tag{2.22}$$

Putting (2.22) into (2.18) gives

$$\int_0^L EI(x)\frac{d^2Y_r(x)}{dx^2}\frac{d^2Y_s(x)}{dx^2} = \omega_r^2\int_0^L m(x)Y_s(x)Y_r(x)\,dx \tag{2.23}$$

Similarly multiplying 2.19 with $Y_r(x)$ and integrating over L with same procedures (2.20) becomes

15

$$\int_0^L EI(x) \frac{d^2 Y_r(x)}{dx^2} \frac{d^2 Y_s(x)}{dx^2} = \omega_s^2 \int_0^L m(x) Y_s(x) Y_r(x)\, dx \qquad (2.24)$$

Subtracting (2.24) from (2.23)

$$(w_r^2 - w_s^2) \int_0^L m(x) Y_s(x) Y_r(x)\, dx = 0 \qquad (2.25)$$

So for distinct solutions, $w_r \neq w_s$ then this states that

$$\int_0^L m(x) Y_s(x) Y_r(x)\, dx = 0, \qquad r \neq s \qquad (2.26)$$

And from (2.18) it can be written that

$$\int_0^L Y_s(x) \frac{d^2}{dx^2} \left[EI(x) \frac{d^2 Y_r(x)}{dx^2} \right] dx = 0, \qquad r \neq s \qquad (2.27)$$

When r=s, equation (2.26) and (2.27) are not zero, and $Y(x)$ can be such that (2.26) and (2.27) becomes

$$\int_0^L m(x) Y_r(x) Y_r(x)\, dx = 1, r = 1,2, \dots \qquad (2.28)$$

$$\int_0^L Y_r(x) \frac{d^2}{dx^2} \left[EI(x) \frac{d^2 Y_r(x)}{dx^2} \right] dx = \omega_r^2, \qquad r = 1,2, \dots \qquad (2.29)$$

Then it is possible to write from equations (2.28) and (2.29) the expansion theorem as

"Any function Y(x) representing a possible displacement of the beam, which implies that Y(x) satisfies boundary conditions of the problem and is such that $(d^2/dx^2)(EI(x)d^2Y(x)/dx^2]$ is continuous, can be expanded in the absolutely and uniformly convergent series of the eigenfunctions

$$Y(x) = \sum_{r=1}^{\infty} c_r Y_r(x) \qquad (2.30)$$

Where the constant coefficients cr are defined by

$$c_r = \int_0^L m(x)Y_s(x)Y(x)\,dx, \qquad r = 1,2,\dots \tag{2.31}$$

And

$$\omega_r^2 c_r = \int_0^L Y_r(x)\frac{d^2}{dx^2}\left[EI(x)\frac{d^2Y(x)}{dx^2}\right]dx, \qquad r = 1,2,\dots " \tag{2.32}$$

This states that any arbitrary displacement of the beam can be written as a sum of its eigenfunctions and its response to initial conditions or external forces can be calculated.

2.4 Modal Domain Representation

The expansion theorem does not cover time response of the beam. For the beam equation assume a solution for $y(x,t)$ in the following form

$$y(x,t) = \sum_{r=1}^{\infty} \phi_r(x)\eta_r(t) \tag{2.33}$$

Where ϕ_r is the mass normalized modes of the system and $\eta_r(t)$ are time dependent functions. Then placing (2.33) into (2.1) yields

$$-\sum_{r=1}^{\infty}\frac{d^2}{dx^2}\left[EI(x)\frac{d^2\phi_r(x)}{dx^2}\right]\eta_r(t) = \sum_{r=1}^{\infty} m(x)\phi_r(x)\frac{d^2\eta_r(t)}{dt^2}, \tag{2.34}$$
$$0 < x < L$$

Then multiply (2.34) by ϕ_s and integrate over L

$$-\sum_{r=1}^{\infty}\int_0^L\left\{\phi_s(x)\frac{d^2}{dx^2}\left[EI(x)\frac{d^2\phi_r(x)}{dx^2}\right]dx\right\}\eta_r(t)$$

$$= \sum_{r=1}^{\infty}[\int_0^L m(x)\phi_s(x)\phi_r(x)dx]\frac{d^2\eta_r(t)}{dt^2} \tag{2.35}$$

From the orthonormality equations (2.26)-(2.29) we obtain the independent set of modal equations.

$$\ddot{\eta}_r(t) + \omega_r^2\eta_r(t) = 0, \qquad r = 1,2\dots \tag{2.36}$$

Here, r represents the modal coordinate index. And the transformation between real coordinates and modal coordinates are defined with the equation (2.33).

Equation (2.36) states that in the modal domain every mode is a single degree of freedom system and its solution is analogous to the solution of a SDOF system. Free vibration oscillations can be written as

$$\eta_r = C_r \cos(w_r t - \theta_r) = \eta_r(0)\cos w_r t + \frac{\dot\eta_r(0)}{w_r}\sin w_r t,$$
$$r = 1,2,\dots \tag{2.37}$$

Where the modal initial conditions can be calculated from real initial conditions

$$\eta_r(0) = \int_0^L m(x)\phi_r(x)y_0(x)dx \ , r = 1,2,\dots \tag{2.38}$$

$$\dot\eta_r(0) = \int_0^L m(x)\phi_r(x)v_0(x)dx \ , r = 1,2,\dots \tag{2.39}$$

The above procedure is only shown for the case of a simply supported beam but the same procedure can be repeated for other type of structures.

2.5 Response to External Excitation

After obtaining the response of a structure to initial conditions, the response to an external excitation will be shown.

Rewriting the equation (2.1) with forcing function f(x,t) yields

$$-\frac{\partial^2}{\partial x^2}\left[EI(x)\frac{\partial^2 y(x,t)}{\partial x^2}\right] + f(x,t) = m(x)\frac{\partial^2 y(x,t)}{\partial t^2} \tag{2.40}$$

Then repeating the process from (2.2) to (2.36) , (2.36) modal equation is modified to

$$\ddot\eta_r(t) + \omega_r^2\eta_r(t) = N_r(t), \qquad r = 1,2\dots \tag{2.41}$$

Where

$$N_r(t) = \int_0^L \phi_r(x)f(x,t)dx \ , \qquad r = 1,2,\dots \tag{2.42}$$

Assume that the forcing function is a point force applied at x_f which can be written as

$$f(x,t) = \delta(x - x_f)F(t) \tag{2.43}$$

Where

$$\delta(x - x_f) = 1 \ when \ x = x_f \tag{2.44}$$

$$\delta(x - x_f) = 0 \ when \ x \neq x_f \tag{2.45}$$

Then the integration at (2.42) reduces to

$$N_r(t) = \phi_r(x_f)F(t) \tag{2.46}$$

And for point force modal equation can be written as

$$\ddot{\eta}_r(t) + \omega_r^2 \eta_r(t) = \phi_r(x_f)F(t), \qquad r = 1,2 \dots \tag{2.47}$$

This concludes the undamped equation for the state space representation of a structure with a point force acting at point f.

2.6 Systems with Proportional Modal Damping

To complete the formulation, damping needs to be added to the model. Up to this point, it is shown that a structure can be modelled as a sum of infinite number of single degree of freedom systems in modal domain with modal mass and modal stiffness.

For an SDOF system, a damping ratio of ζ_r for the rth mode can be implemented into the equation (2.47) analogous to SDOF vibratory systems as

$$\ddot{\eta}_r(t) + 2\omega_r \zeta_r \dot{\eta}(t) + \omega_r^2 \eta_r(t) = \phi_r(x_f)F(t),$$
$$r = 1,2 \dots \tag{2.48}$$

Damping of a structure can be found experimentally or it can be based the material properties of the structure and obtained from the literature.

2.7 Transient and steady state response

To compare the state space model with analytical model an analytical solution is necessary. Every mode is decoupled from each other therefore each modes response can be calculated as SDOF system and summed up to find the final response. It is not possible to sum up infinite modes so it is truncated to finite number of modes.

19

Response of a differential system composes of transient and steady state solutions. The solutions can be written as [32]

$$\eta_r(t) = e^{-\zeta_r \omega_r t}\left(A_r \, sin(\omega_r^d t) + B_r cos(\omega_r^d t)\right)$$
$$+ X_r sin(\Omega t - \theta) \quad r = 1,2 \dots \tag{2.49}$$

Where

$$X_r = \frac{F_o \phi_r(x_f)}{\sqrt{(\omega_r^2 - \Omega^2)^2 + (2\zeta_r \omega_r \Omega)^2}} \tag{2.50}$$

F_0 is the amplitude of the harmonic excitation.

Damped natural frequency is defined as

$$\omega_r^d = \omega_r \sqrt{1 - \zeta_r^2} \tag{2.51}$$

A_r and B_r can be found by implementing initial conditions. Transformation between physical domain and modal domain can be done by equations (2.52) and (2.39).

θ if found by the following equation

$$\tan(\theta_r) = \frac{2\zeta_r \omega_r \Omega}{\omega_r^2 - \Omega^2} \tag{2.52}$$

After obtaining response for each mode, by using equation (2.33) physical response can be found.

2.8 State Space Representation of a 1D Structure with Point Force

State space representation of a system can be shown as

$$\dot{x} = Ax + Bu \tag{2.53}$$

$$y = Cx + Du \tag{2.54}$$

Where x is the chosen states of the system, u is the external force vector, y is the chosen outputs for the system. A, B, C, D are the matrices that defines the system dynamics.

Equation (2.52) can be used to write the decoupled modal equations in state space. Let the modal displacement be defined by η and modal velocity by $\dot{\eta}$. In

20

the previous analysis it is shown that the response of a structure is infinite sum of its modal domain SDOF responses. However, in real case it is necessary to truncate it to a finite number of modes. Let the number of modes used in the series summation is m and number of forces are f. Then, states and their derivatives can be written respectively as

$$x = [\eta_1 \ \eta_2 \ ... \eta_m \ \dot{\eta}_1 \ \dot{\eta}_2 \ ... \ \dot{\eta}_m]^T_{2mx1} \tag{2.55}$$

$$\dot{x} = [\dot{\eta}_1 \ \dot{\eta}_2 \ ... \ \dot{\eta}_m \ \ddot{\eta}_1 \ \ddot{\eta}_2 \ ...\ddot{\eta}_m \ ]^T_{2mx1} \tag{2.56}$$

The normalized mode shape functions are defined as

$$\Phi(x) = [\phi_1(x) \quad \phi_2(x) \quad ... \quad \phi_m(x)]_{1xm} \tag{2.57}$$

Considering equation (2.52) and re-writing it in the appropriate format

$$\ddot{\eta}_r(t) = -2\omega_r\zeta_r\dot{\eta}(t) - \omega_r^2\eta_r(t) + \phi_r(x_1)F_1(t) + \phi_r(x_2)F_2(t)$$
$$+ \cdots + \phi_r(x_f)F_f(t), \qquad r = 1,2 \tag{2.58}$$

Then the A and B matrices can be written as

$$A = \begin{bmatrix} \mathbf{0}_{mxm} & I_{mxm} \\ -\omega^2_{mxm} & -2\zeta\omega_{mxm} \end{bmatrix}_{2mx2m} \tag{2.59}$$

$$B = \begin{bmatrix} \mathbf{0}_{mxf} \\ \Phi^T(x_1) \ \Phi^T(x_2) \ ... \ \Phi^T(x_f) \end{bmatrix}_{2mxf} \tag{2.60}$$

And $\omega^2, -2\zeta\omega$ and u can be written as

$$u = [F_1(t) \ F_2(t) \ ... \ F_f(t)]^T_{fx1} \tag{2.61}$$

$$\omega^2 = \begin{bmatrix} \omega_1^2 & 0 & ... & 0 \\ 0 & \omega_2^2 & ... & ... \\ ... & ... & ... & 0 \\ 0 & ... & 0 & w_m^2 \end{bmatrix}_{mxm} \tag{2.62}$$

$$-2\zeta\omega = \begin{bmatrix} -2\zeta_1\omega_1 & 0 & ... & 0 \\ 0 & -2\zeta_2\omega_2 & ... & ... \\ ... & ... & ... & 0 \\ 0 & ... & 0 & -2\zeta_m w_m \end{bmatrix}_{mxm} \tag{2.63}$$

21

This concludes the definition of A and B matrices. Outputs are the displacement, velocity or acceleration of an arbitrary point defined in the domain of the structure. Then to find the displacements, equation (2.33) is re-written.

$$y(x,t) = \sum_{r=1}^{\infty} \phi_r(x)\eta_r(t) \tag{2.64}$$

Taking the derivative with respect to time will yield the velocity of a point.

$$\dot{y}(x,t) = \sum_{r=1}^{\infty} \phi_r(x)\dot{\eta}_r(t) \tag{2.65}$$

It is possible to write y(x,t) and $\dot{y}(x,t)$ in terms of the states $\eta, \dot{\eta}$. To find the acceleration one more derivative is taken with respect to time.

$$\ddot{y}(x,t) = \sum_{r=1}^{\infty} \phi_r(x)\ddot{\eta}_r(t) \tag{2.66}$$

$\ddot{\boldsymbol{\eta}}$ is not one of the states. Then it is necessary to write it in terms of $\boldsymbol{\eta} \ and \ \dot{\boldsymbol{\eta}}$. From equation (2.53) it is known that

$$\ddot{\eta}_r(t) = -2\zeta_r\omega_r - \omega_r^2\eta_r(t) + \phi_r(x_1)F_1(t) + \phi_r(x_2)F_2(t) + \cdots \\ + \phi_r(x_f)F_f(t), \qquad r = 1,2 \tag{2.67}$$

Then placing (2.58) into (2.66) the acceleration can be found in terms of our states and external excitations. To find the y given below, the C and D matrix can be written in general form as

$$\boldsymbol{y_k} = [y(x_k,t) \ \ \dot{y}(x_k,t) \ \ \ddot{y}(x_k,t)]^T \tag{2.68}$$

$$\boldsymbol{C} = \begin{bmatrix} \boldsymbol{\Phi(x_k)_{1xm}} & \boldsymbol{0_{1xm}} \\ \boldsymbol{0_{1xm}} & \boldsymbol{\Phi(x_k)_{1xm}} \\ -\boldsymbol{\omega^2\Phi(x_k)_{1xm}} & -\boldsymbol{2\zeta\omega\Phi(x_k)_{1xm}} \end{bmatrix}_{3x2m} \tag{2.69}$$

$$\boldsymbol{D} = \begin{bmatrix} \boldsymbol{0_{1xf}} \\ \boldsymbol{0_{1xf}} \\ \Phi(x_k)_{1xm}[\Phi^T(x_1) \ \Phi^T(x_2) \dots \Phi^T(x_f)]_{mxf} \end{bmatrix}_{3xf} \tag{2.70}$$

2.9 Numerical Example

2.9.1 Problem Definition

The state space representation with 5 modes will be compared with the analytical formulation result with 5 modes of a simply supported beam with the following properties

Length: 1 meter

Width: 0.1 meters

Height: 0.01 meters

Excitation point, $x_f = 0.3$ meter

Excitation frequency: $\Omega = 10$ Hz, 50 Hz

Required response is at $x = 0.5$ meter

Damping: 5% to each mode

Number of modes: 5

Then the required parameters can be calculated as

L = 1 m

E = 70 GPa

$I = 8.33 \times 10\text{-}9 \text{ m}^4$

m = 2.7 kg/m

The normalized mode shapes for simply supported beam are

$$\phi_r(x) = \sqrt{\frac{2}{mL}} \sin \frac{r\pi x}{L}, \qquad r = 1, 2, \dots, m$$

The natural frequencies are

$$\omega_r = (r\pi)^2 \sqrt{\frac{EI}{mL^4}}$$

A MATLAB model is created with both analytical formulation and state space formulation. A simulink model is done to see the results. Simulink model is shown in the figure 2.3
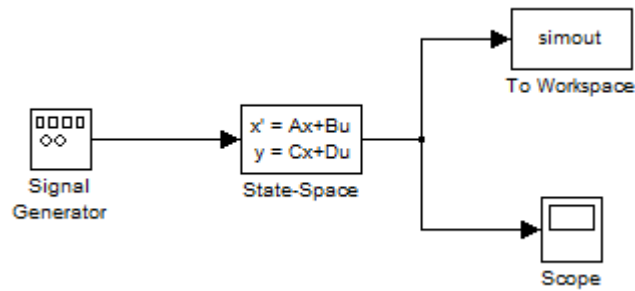
Figure 2-3 - Simulink Model of Open Loop State Space System

As 5 modes are modelled in the simulation, one should determine the step size accordingly. 5th mode is at 577 Hz, then a step size of 10^{-4} is selected. For analytical model directly MATLAB is used. For state space model fixed-step size ode8 solver is used.

2.9.2   Results

The result for 10 Hz excitation and 50 Hz excitation is shown below.
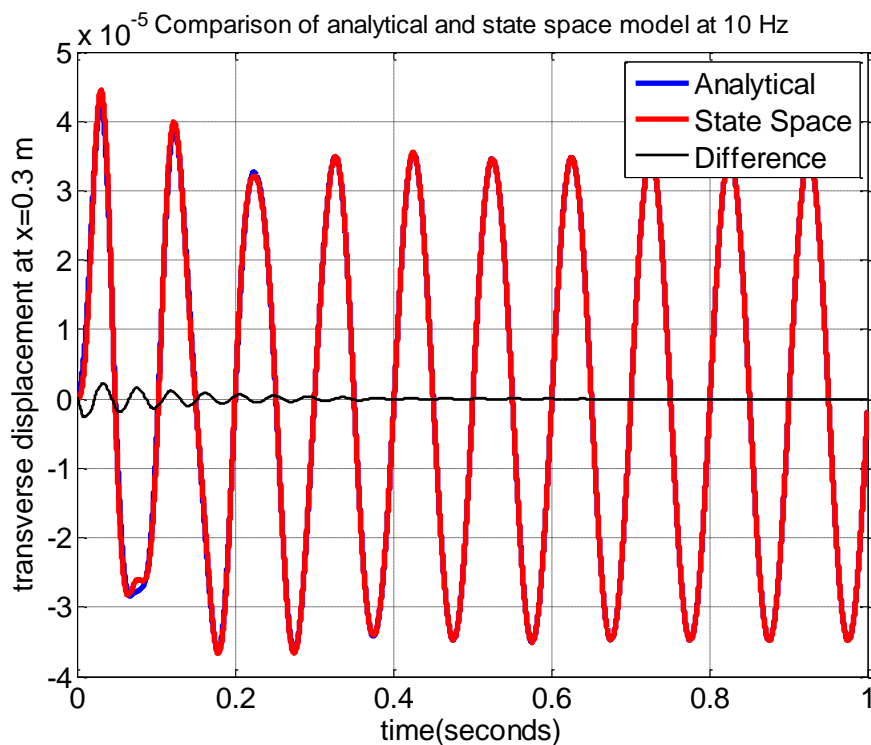
Figure 2-4 Simply Supported Beam Response to 10 Hz Excitation
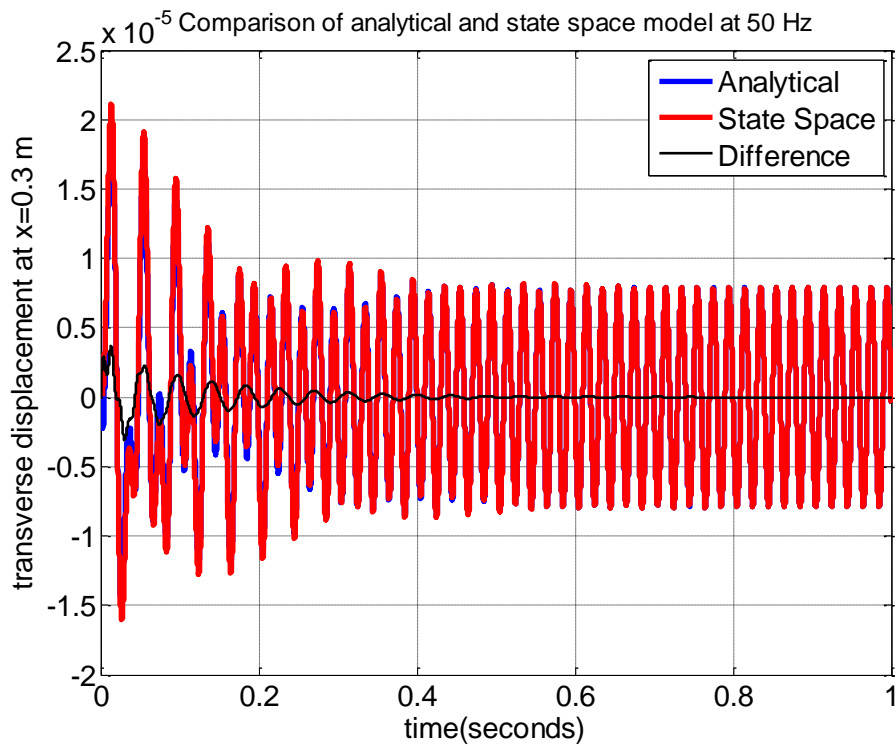
Figure 2-5 Simply Supported Beam Response to 50 Hz Excitation

2.10 Numerical Example II

By applying step input and waiting appropriate time to damp out transient response one should obtain steady state static deflection. Also static deflection of a simply supported beam is also analytically known From [33] for an intermediate load the scheme is
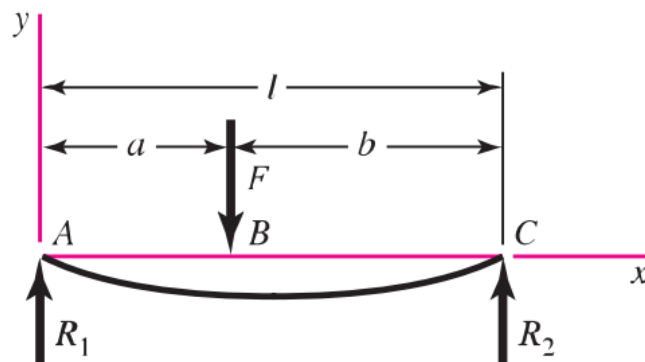
Figure 2-6 Simply Supported Beam Intermediate Load Static Deflection

And for the deflection between B and C is defined as

$$y = \frac{Fa(l-x)}{6EIl}(x^2 + a^2 - 2lx) \qquad (2.71)$$

The geometry, boundary conditions and material is same as the Section 2.8. A step force is applied at 0.3 meters and the deflection at 0.5 meters is sought. Then

$$a = 0.3\ m, x = 0.5\ m, F = 1N, l = 1\ m, EI = 583.1\ Nm^2$$

Then by placing the values the deflection is found as

$$y = -2.8297 * 10^{-5}\ m$$

Simply supported beam with same properties and same force properties is modelled in Matlab and simulated by Simulink. The state space result is given in Figure 2-6. The steady state response is $2.828 * 10^{-5}\ m$ and error between analytical formulation and state space representation is 0.06%.
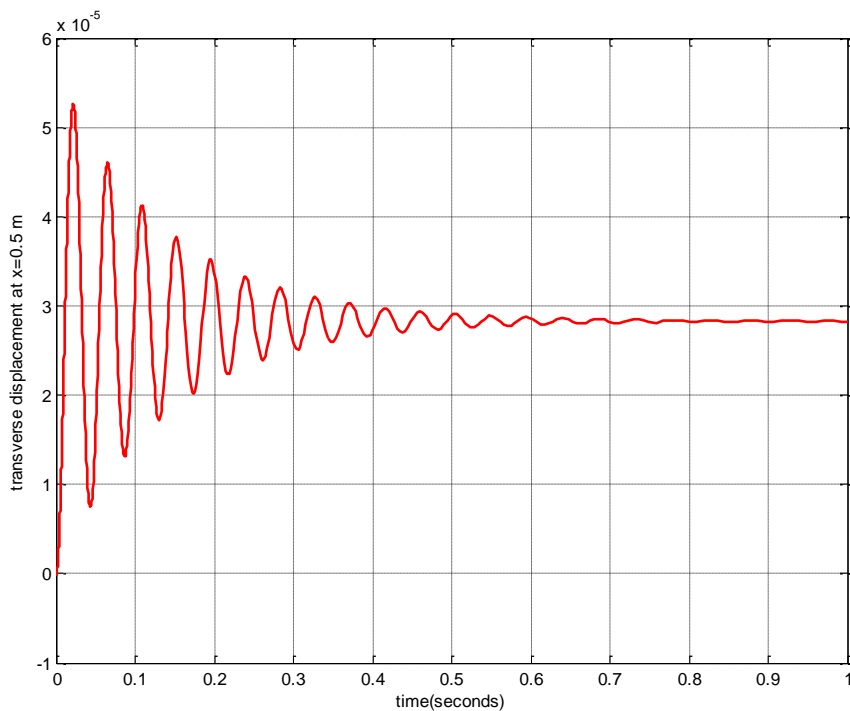
Figure 2-7 Simply Supported Beam Response to Step Input and Steady State Result

CHAPTER 3

DISCRETIZATION AND GENERALIZATION OF STATE SPACE MODEL

3.1 Introduction

In Chapter 2 it is shown that a distributed structure can be modelled in state space as the sum of its normalized modes. It is possible to model rods, strings, beams and plates with the analytical models that are available in the literature. However, most of the structures that are used in real life does not have any analytical model. To overcome this problem, Finite Element Analysis (FEA) is widely used. In FEA a structure is divided into finite number of structural elements and the solution for displacement, velocity, temperature etc. is found numerically. In our case it is required to find mode shape vectors, natural frequencies, modal masses and modal stiffnesses.

3.2 Discretizing the 1D State Space Model

Only difference between distributed model and discrete model is in terms of mode shape definition. In continuous analysis mode shapes are functions that are expressed analytically. In the discretized structures mode shape vectors are used. The vectors are analogous to continuous shape functions, in fact the values are pre-calculated at nodes of the structure.

In Chapter 2, it is shown that for the case with excitation using point forces it is possible to obtain a state space model. To prevent interpolations in discrete modelling, it is assumed that forces are applied to the nodes of the FEM. Furthermore, the responses are also calculated at the nodes. With the above differences in mind, A, B, C, D matrices should be rewritten for a discrete case. The definition for the mode shape vector for r$^{\text{th}}$ mode is given as

$$\boldsymbol{\phi_r} = [\phi_r(1)\ \phi_r(2) \dots \phi_r(n)]_{nx1}^T \tag{3.1}$$

Where n is the number of nodes in the structure. The mode shape matrix is written as

$$\boldsymbol{\Phi} = [\boldsymbol{\phi_1}\ \boldsymbol{\phi_2} \dots \boldsymbol{\phi_m}]_{nxm} \tag{3.2}$$

Where m is the number of modes included in the model. Then considering the same process given in Section 2.7 A, B, C, D are the same. However it is necessary to choose the points such that they are coincident with the nodes of the FEA. Also it should be noted that

$$\Phi(x) = [\phi_1(x)\, \phi_2(x) \ldots \phi_m(x)]_{1xm} \tag{3.3}$$

And x is the selected node number. Therefore instead of using physical coordinates to evaluate mode shape function now the values directly at the selected node is used the equations.

3.3 Generalized State Space Approach in 3D

In the literature survey it is shown that modal space approach is used on cantilever beams and plate type structures. However it is not common to use this approach for three dimensional structures. The formulation given in Section 3-1 and 3.3 will be expanded for three dimensional structures in this section.

In addition to m and n, the number of modes included in the model and number of nodes of FEA, a new abbreviation d is added to the formulation which is the number of degrees of freedom of a structure. It is taken as six in the formulation as a point can translate in three directions and can rotate about three axes.

Mode shape vector is written in the form given in Eqn. 3.4. Subscripts denote the mode number and superscripts denotes the mode shape vector at that degree of freedom.

$$\phi_i = \begin{bmatrix} \phi_i^x \\ \phi_i^y \\ \phi_i^z \\ \phi_i^{rotx} \\ \phi_i^{roty} \\ \phi_i^{rotz} \end{bmatrix}_{(d*n)x1} \tag{3.4}$$

And the mode shape matrix is written as

$$\Phi = [\phi_1\, \phi_2 \ldots \phi_{m-1} \phi_m]_{(d*n)xm} \tag{3.5}$$

States are same as before, modal displacements and modal velocities.

$$x = [\eta_1 \ \eta_2 \ ... \eta_m \ \dot{\eta}_1 \ \dot{\eta}_2 \ ... \ \dot{\eta}_m]^T_{2mx1} \tag{3.6}$$

A matrix is same as before as it does not include any mode shapes term. Only natural frequencies and modal damping ratios are included.

B matrix is expanded to include all the information about every node. To find **B** matrix we need to first obtain input vector **u**. At every node, three forces and three moments can be applied. Therefore the size of the matrix is d*n x 1. Subscripts denote the node number and superscripts denote the degree of freedom. *F* is for forces and *M* is for moments.

$$\boldsymbol{u} = \left[F_1^x..F_n^x \ F_1^y..F_n^y \ F_1^z..F_n^z \ M_1^x..M_n^x \ M_1^y..M_n^y..M_1^z..M_n^z\right]^T_{dn \ x \ 1} \tag{3.7}$$

$$B = \begin{bmatrix} \mathbf{0}_{mx1} \\ \phi_1^T \\ \phi_2^T \\ ... \\ \phi_{m-1}^T \\ \phi_m^T \end{bmatrix}_{(2m) \ x \ (dn)} \tag{3.8}$$

y vector is the output vector. It contains the information of displacement, velocity and acceleration of every node in every direction. (6 degrees of freedom). Therefore the number of elements in it is 3*n*d. Its dimensions are (3*n*d) x 1. The coding is given below. Subscripts are used for node number.

$$x = [x_1 \ x_2 \ ... x_n]^T_{nx1} \qquad \dot{x} = [\dot{x}_1 \ \dot{x}_2 \ ... \dot{x}_n]^T_{nx1} \qquad \ddot{x} = [\ddot{x}_1 \ \ddot{x}_2 \ ... \ddot{x}_n]_{nx1}$$

$$y = [y_1 \ y_2 \ ... y_n]^T_{nx1} \qquad \dot{y} = [\dot{y}_1 \ \dot{y}_2 \ ... \dot{y}_n]^T_{nx1} \qquad \ddot{y} = [\ddot{y}_1 \ \ddot{y}_2 \ ... \ddot{y}_n]_{nx1}$$

$$z = [z_1 \ z_2 \ ... z_n]^T_{nx1} \qquad \dot{z} = [\dot{z}_1 \ \dot{z}_2 \ ... \dot{z}_n]^T_{nx1} \qquad \ddot{z} = [\ddot{z}_1 \ \ddot{z}_2 \ ... \ddot{z}_n]_{nx1}$$

$$(3.9a\text{-}3.9i)$$

$$\boldsymbol{rotx} = [rotx_1 \; rotx_2 \; ... \; rotx_n]^T{}_{nx1} \tag{3.10a}$$

$$\boldsymbol{\dot{rotx}} = [\dot{rotx}_1 \; \dot{rotx}_2 \; ... \; \dot{rotx}_n]^T{}_{nx1} \tag{3.10b}$$

$$\boldsymbol{\ddot{rotx}} = [\ddot{rotx}_1 \; \ddot{rotx}_2 \; ... \; \ddot{rotx}_n]_{nx1} \tag{3.10c}$$

$$\boldsymbol{roty} = [roty_1 \; roty_2 \; ... \; roty_n]^T{}_{nx1} \tag{3.10d}$$

$$\boldsymbol{\dot{roty}} = [\dot{roty}_1 \; \dot{roty}_2 \; ... \; \dot{roty}_n]^T{}_{nx1} \tag{3.10e}$$

$$\boldsymbol{\ddot{roty}} = [\ddot{roty}_1 \; \ddot{roty}_2 \; ... \; \ddot{roty}_n]_{nx1} \tag{3.10f}$$

$$\boldsymbol{rotz} = [rotz_1 \; rotz_2 \; ... \; rotz_n]^T{}_{nx1} \tag{3.10g}$$

$$\boldsymbol{\dot{rotz}} = [\dot{rotz}_1 \; \dot{rotz}_2 \; ... \; \dot{rotz}_n]^T{}_{nx1} \tag{3.10h}$$

$$\boldsymbol{\ddot{rotz}} = [\ddot{rotz}_1 \; \ddot{rotz}_2 \; ... \; \ddot{rotz}_n]_{nx1} \tag{3.10i}$$

$$Y = \begin{bmatrix} x \\ y \\ z \\ rotx \\ roty \\ rotz \end{bmatrix}_{(d*n) \, x \, 1} \quad \dot{Y} = \begin{bmatrix} \dot{x} \\ \dot{y} \\ \dot{z} \\ \dot{rotx} \\ \dot{roty} \\ \dot{rotz} \end{bmatrix}_{(d*n) \, x \, 1} \quad \ddot{Y} = \begin{bmatrix} \ddot{x} \\ \ddot{y} \\ \ddot{z} \\ \ddot{rotx} \\ \ddot{roty} \\ \ddot{rotz} \end{bmatrix}_{(d*n) \, x \, 1} \tag{3.11}$$

$$y = \begin{bmatrix} Y \\ \dot{Y} \\ \ddot{Y} \end{bmatrix}_{(3*d*n) \, x \, 1} \tag{3.12}$$

With the given $\boldsymbol{y}$ vector $\boldsymbol{C}$ and $\boldsymbol{D}$ matrices can be revised. The total displacements, velocities and accelerations can be obtained by modal superposition. Superposition is shown below.

$$y(x_1, t) = \phi_1(x_1)\eta_1(t) + \phi_2(x_1)\eta_2(t) + \cdots + \phi_{m-1}(x_1)\eta_{m-1}(t)$$
$$+ \phi_m(x_1)\eta_m(t)$$
$$\dot{y}(x_1, t) = \phi_1(x_1)\dot{\eta}_1(t) + \phi_2(x_1)\dot{\eta}_2(t) + \cdots + \phi_{m-1}(x_1)\dot{\eta}_{m-1}(t)$$
$$+ \phi_m(x_1)\dot{\eta}_m(t)$$

$$\ddot{y}(x_1, t) = \phi_1(x_1)\ddot{\eta}_1(t) + \phi_2(x_1)\ddot{\eta}_2(t) + \cdots + \phi_{m-1}(x_1)\ddot{\eta}_{m-1}(t)$$
$$+ \phi_m(x_1)\ddot{\eta}_m(t)$$

<div align="center">(3.13a-3.13c)</div>

By expanding this to matrix form

$$Y = \phi[\eta_1 \; \eta_2 \; ... \; \eta_m]^T \tag{3.14}$$

As velocities are also out states

$$\dot{Y} = \phi[\eta_{m+1} \; \eta_{m+2} \; ... \; \eta_{2m}]^T \tag{3.15}$$

To find accelerations firstly rewrite the modal equation

$$\ddot{\eta}_r(t) = -2\omega_r\zeta\dot{\eta}_r(t) - \omega_r^2\eta_r(t) + \phi_r(x_f)F_r(t) \tag{3.16}$$

Revise the forcing section to be general similar to u vector at (3.7) contains all the forces and moments.

$$\ddot{\eta}_r(t) = -2\omega_r\zeta\dot{\eta}_r(t) - \omega_r^2\eta_r(t) + \phi_r^T u(t) \tag{3.17}$$

Then multiplying (3.17) with ϕ will give the accelerations. From here C and D matrices can be obtained as following.

$$C = \begin{bmatrix} \Phi & 0_{dnxm} \\ 0_{dnxm} & \Phi \\ -\Phi\omega^2 & -2\Phi\zeta\omega \end{bmatrix}_{3dnx2m} \tag{3.18}$$

$$D = \begin{bmatrix} 0_{dnxdn} \\ 0_{dnxdn} \\ \Phi\Phi^T \end{bmatrix}_{3dnxdn} \tag{3.19}$$

With those A, B, C, and D matrices any structure with 3D FEA can be modeled in state space.

3.4 Reducing the size of B, C, D Matrices

Calculated B, C, D matrices obtain data about every node. However in real case information on B matrix should only contain the actuated node and C & D matrices should only contain information of the nodes with sensors. Then controllability and observability matrices can be correctly found.

Assuming there are f number of actuators. $\boldsymbol{B}$ matrix should reduce from (2m x dn) to (2m x f) size such that $\boldsymbol{u}$ vector is size of (f x 1). Then to eliminate the unnecessary information from $\boldsymbol{B}$ matrix, lower side of $\boldsymbol{B}$ matrix is multiplied with a matrix $\boldsymbol{E_f}$ size of (dn x f). $\boldsymbol{E_f}$ is a 0 matrix except 1 is placed at (d(w)*n(w),w), where w stands for point forces starting from 1 to f. d(w) stands for the corresponding degree of freedom of the actuator and n is the corresponding node number. $\boldsymbol{B}$ matrix is written as

$$B = \begin{bmatrix} \boldsymbol{0}_{mx1} \\ \boldsymbol{\Phi}^T * \boldsymbol{E_f} \end{bmatrix}_{(2m) \; x \; (f)} \tag{3.20}$$

Similar approach can be done for $\boldsymbol{C}$ and $\boldsymbol{D}$ matrices. Assume that dis is the number of displacement sensors, vel is the number of velocity sensors and acc is the number of acceleration sensors. $\boldsymbol{E_d}, \boldsymbol{E_v}, \boldsymbol{E_a}$ are the corresponding matrices with size of (dis x d*n), (vel x d*n), (acc x d*n). $\boldsymbol{C}$ and $\boldsymbol{D}$ matrices can be written at reduced form as

$$C = \begin{bmatrix} \mathbf{E_d}\boldsymbol{\Phi} & \boldsymbol{0}_{dnxm} \\ \boldsymbol{0}_{dnxm} & \mathbf{E_v}\boldsymbol{\Phi} \\ -E_a\boldsymbol{\Phi}\omega^2 & -E_a 2\boldsymbol{\Phi}\zeta\omega \end{bmatrix}_{(dis+vel+acc)x2m} \tag{3.21}$$

$$D = \begin{bmatrix} \boldsymbol{0}_{disxdn} \\ \boldsymbol{0}_{velxdn} \\ \mathbf{E_d}\boldsymbol{\Phi}\boldsymbol{\Phi}^T E_a \end{bmatrix}_{(dis+vel+acc)xdn} \tag{3.22}$$

$\boldsymbol{E_d}$ is a zero matrix except (@dis, d(@dis)*n(@dis)) = 1. @dis corresponds for the number of the sensor from 1 to dis and d(@dis) gives the degree of freedom displacement sensor and n(@dis) gives the node of displacement sensor. $\boldsymbol{E_v}$ and $\boldsymbol{E_a}$ sensors can be found with same procedure for velocity and acceleration sensors.

3.5 Discrete Simply Supported Beam Compared With the Continuous Model

For the same beam given in Section 2.8 a finite element analysis has been done using NASTRAN/PATRAN. Beam is discretized into 20 one dimensional beam

elements with 21 nodes. Each node is uniformly distributed from each other. Length of the beam is 1 meter. Distance between nodes are 0.05 m. This suggests that one must choose the actuator points or sensor points at those intervals. The nodes of the beam are shown in Figure 3.1 below.

Figure 3-1 Simply Supported Beam Model and Node Numbers

One dimensional modal analysis is performed using FEM and the resulting mode shapes for first three modes are shown in the Figures 3-2 to 3-4. The number on each figure indicates the maximum value for displacement ratio. The mode shapes are mass normalized.

Figure 3-2 First Mode Shape
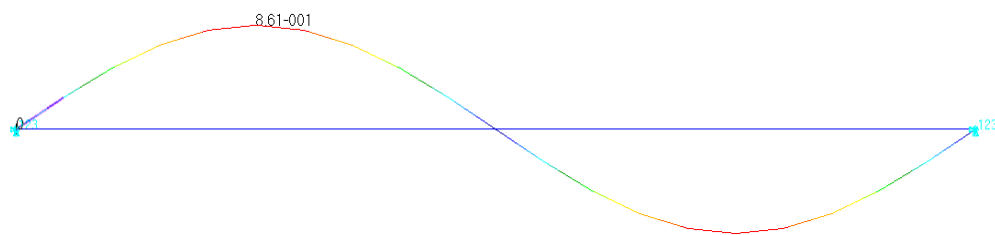
Figure 3-3 Second Mode Shape
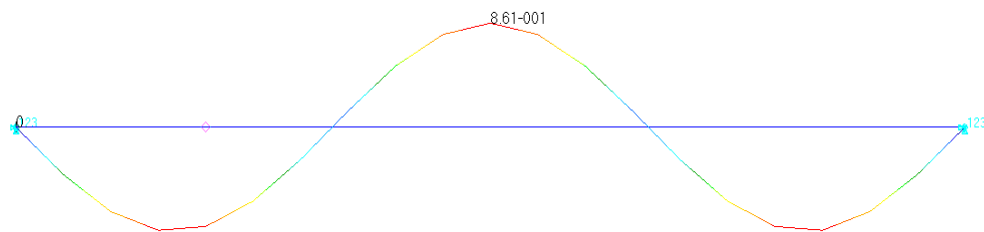
Figure 3-4 Third Mode Shape

For the first eight modes, the natural frequencies are compared with the distributed model in the Table 3.1.

33

Table 3-1 Comparison of Natural Frequencies for Simply Supported Beam

	Discrete Model (Hz)	Distributed Model (Hz)
1st mode	23.086	23.088
2nd mode	92.306	92.354
3rd mode	207.55	207.80
4th mode	368.6	369.4
5th mode	575.12	577.2
6th mode	826.57	831.2
7th mode	1122.11	1131.33
8th mode	1460.6	1477.66

The error is increasing as the modes increase however up to seventh mode absolute error is below 1% and at eighth mode absolute error is 1.15%. In the previous corresponding example, excitation was applied at x=0.3m and response was measured at x=0.5m. Then the mode shape values at those points should be compared with each other before comparing the results. Then for x=0.3m values at seventh node will be taken and compared with continuous model.

Table 3-2 Comparison of Mode Shape Values of Simply Supported Beam

	Discrete Model - $\phi(7)$	Distributed Model $\phi(0.3)$
1st mode	0.696291	0.696290
2nd mode	0.818539	0.818539
3rd mode	0.26596	0.26595
4th mode	-0.505885	-0.505884
5th mode	-0.86066	-0.86066
6th mode	-0.50589	-0.50588
7th mode	0.26596	0.26595
8th mode	0.81854	0.81853

Results are accurate up to 4 digits. Then the same procedure is repeated for x=0.5m. The results are shown in the Table 3.3

Table 3-3 Comparison of Mode Shape Values of Simply Supported Beam

	Discrete Model - $\phi(11)$	Distributed Model $\phi(0.5)$
1st mode	-0.860663	- 0.860662
2nd mode	0	0
3rd mode	0.860663	0.860662
4th mode	0	0
5th mode	0.860663	0.860662
6th mode	0	0
7th mode	-0.86066	-0.860662
8th mode	0	0

The natural frequencies and mode shapes at the given locations are very close to each other. Then it is expected to have similar results. MATLAB and Simulink is used for simulations. 10^{-4} fixed step size is given. For Simulink solution ode5 solver is used. 5% damping is added to the every mode. 8 modes are used, which is up to 1477 Hz.

10 Hz and 50 Hz excitations are considered separately. The results are given below. Difference is the error between Analytical Response and State Space Response
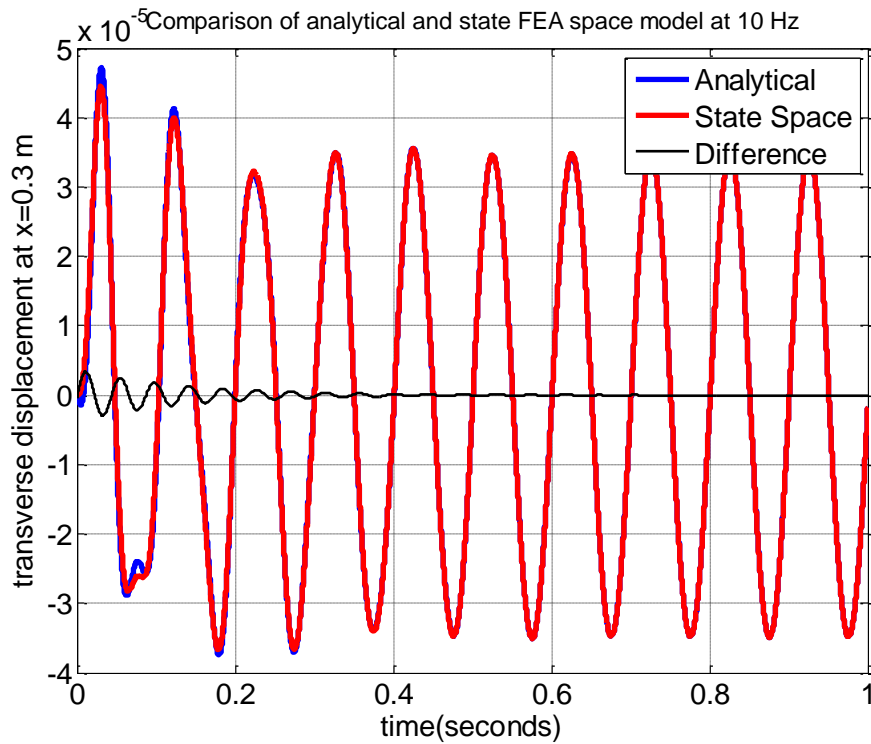
Figure 3-5 Simply Supported Beam Response to 10 Hz sinusoidal excitation
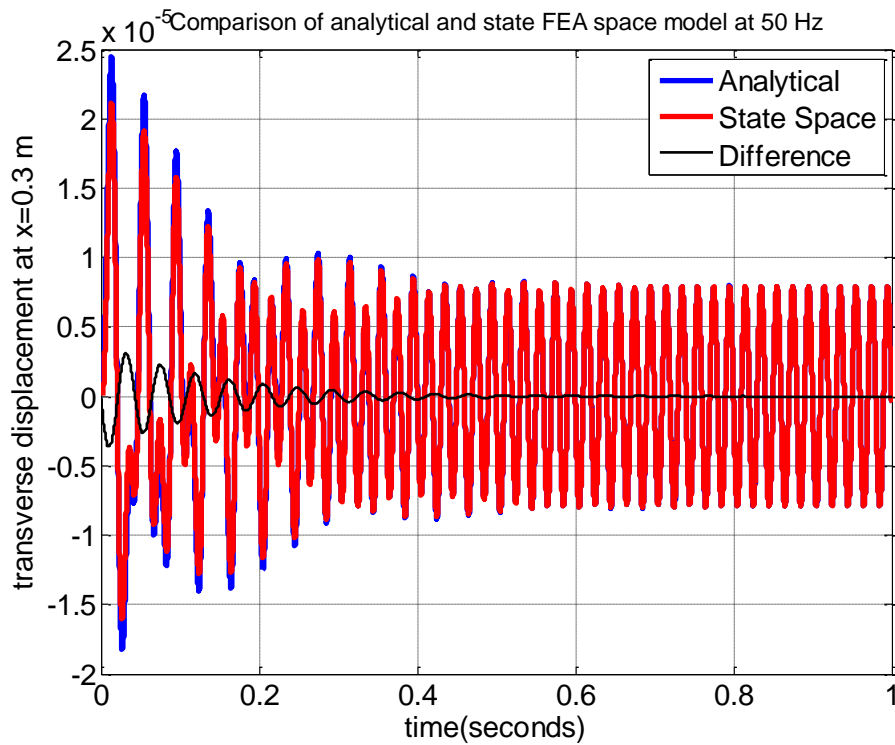
Figure 3-6 Simply Supported Beam Response to 50 Hz sinusoidal excitation

In Figure 3-6 it can be seen that FEA result transient and steady state part is in good agreement with analytical response.

3.6   Numerical Example for Complex Structure

To better evaluate the performance of the state space model, a three dimensional complex shape will be used as a case study. The structure is shown below with the node numbers. The selection of the shape is due to its three dimensional nature. It is modelled with five modes (m=5) 236 nodes (n=236) and three translational degrees of freedom (d=3). It is fixed from the edge of nodes between 1 and 11.
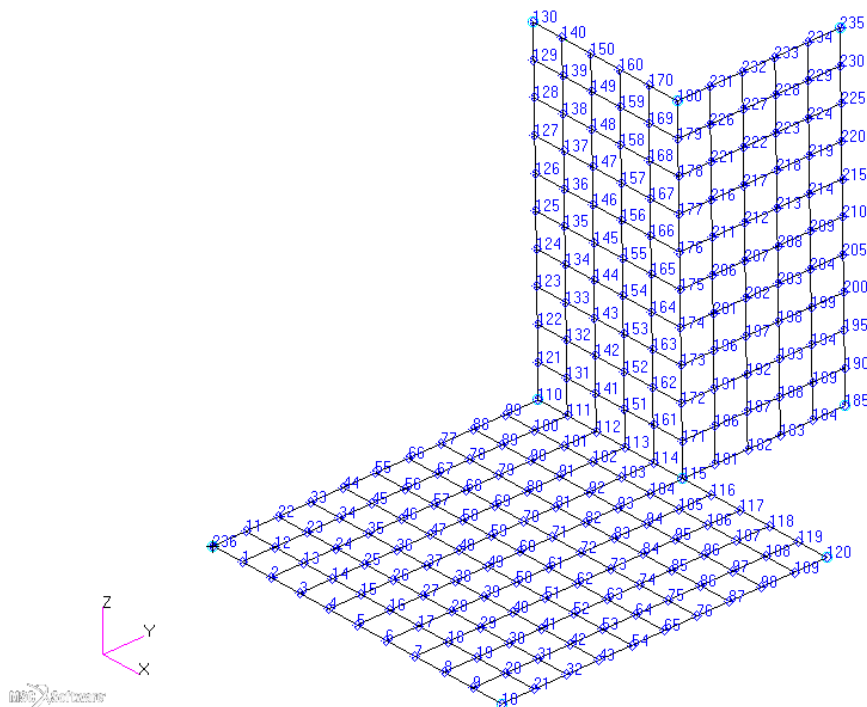
Figure 3-7 Three dimensional complex structure with node numbers

The structure is an aluminum with Young's modulus 70 GPa, density 2700 kg/m^3 and it has a thickness of 2 mm. The long sides are 100 mm and short sides are 50 mm. The first three mode shapes are given below to better visualize the dynamics of the system.

37
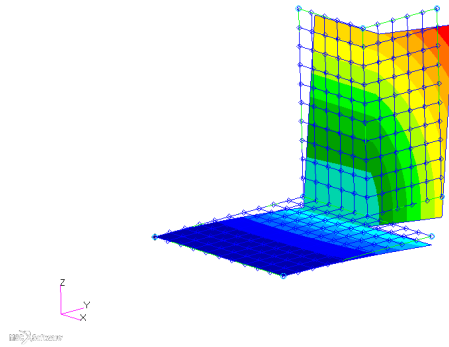
1st mode
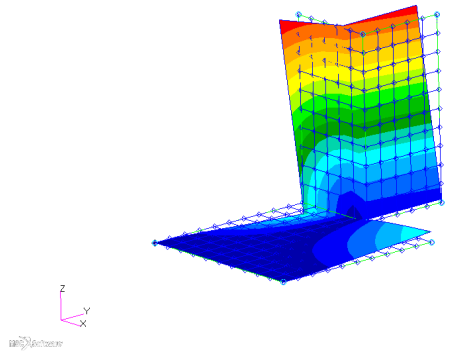
2nd mode
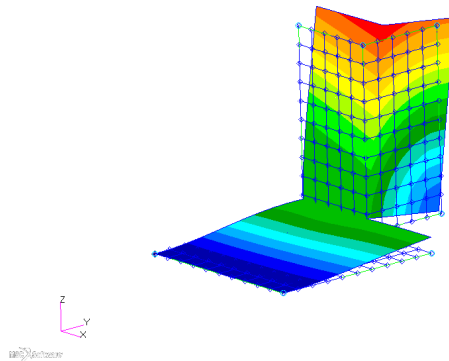
3rd mode

Figure 3-8 First three mode shapes of complex structure

Then assuming that there is an excitation from node 120 in Z direction and accelerometers are located at node 130 in Y direction and at 235 in X direction. The natural frequencies of the system is given in Table 3.4.

Table 3-4 Natural Frequencies of the complex structure

1st mode	48.917 Hz
2nd mode	98.345 Hz
3rd mode	156.46 Hz
4th mode	324.06 Hz
5th mode	619.55 Hz

From here state space matrices A, B, C, and D can be constructed.

A matrix

Assuming that there exists 1% damping for first mode, 2% for second mode and m% for m^{th} mode, diagonal natural frequency and diagonal damping sub-matrices will be defined first.

The natural frequencies of the structure from FEA is shown in Table 3.4 in the form of Hz. It is necessary to convert them to rad/sec and square them. Then the diagonal natural frequency matrix can be found and written below as

$$\omega^2 = \begin{bmatrix} 9.4467e+004 & 0 & 0 & 0 & 0 \\ 0 & 3.8182e+005 & 0 & 0 & 0 \\ 0 & 0 & 9.6642e+005 & 0 & 0 \\ 0 & 0 & 0 & 4.1458e+006 & 0 \\ 0 & 0 & 0 & 0 & 1.5153e+007 \end{bmatrix}$$

Also,

$$2\omega\zeta = \begin{bmatrix} 6.1471 & 0 & 0 & 0 & 0 \\ 0 & 24.7168 & 0 & 0 & 0 \\ 0 & 0 & 58.9840 & 0 & 0 \\ 0 & 0 & 0 & 162.8903 & 0 \\ 0 & 0 & 0 & 0 & 389.2747 \end{bmatrix}$$

and I is 5x5 identity matrix and 0 is 5x5 null matrix. Then A is

$$A = \begin{bmatrix} 0 & I \\ -\omega^2 & -2\omega\zeta \end{bmatrix}$$

B matrix

To define the B matrix, the mode shape values at the 120th node in Z direction must be known first.

Table 3-5 Mode shape values at excitation point

Mode Number	Mode Shape Value at node 120 in Z direction
1st mode	-2.013535
2nd mode	2.597269
3rd mode	3.264399
4th mode	1.182970
5th mode	14.493186

The forcing function u(t) is defined as

$$u(t) = f_1(t)$$

As f_1 is an arbitrary input force. B matrix can be written considering Table 3.5.

$$B = \begin{bmatrix} 0 \\ 0 \\ 0 \\ 0 \\ 0 \\ -2.013535 \\ 2.597269 \\ 3.264399 \\ 1.182970 \\ 14.493186 \end{bmatrix}$$

C matrix

To define the C matrix, the mode shape values of node 130 in Y direction and node 235 in X direction should be written.

Table 3-6 Mode shape values at sensor points

Mode Number	Mode Shape Value at 130th node Y direction	Mode Shape Value at 235th node X direction
1st mode	4.758248	-0.303674
2nd mode	-0.188935	-7.200803
3rd mode	4.694722	-0.890994
4th mode	8.892684	8.593676
5th mode	-2.919328	1.375139

$$\boldsymbol{\phi}_c = \begin{bmatrix} 4.76 & -0.19 & 4.69 & 8.89 & -2.91 \\ -0.30 & -7.20 & -0.89 & 8.59 & 1.38 \end{bmatrix}$$

Then to find the **C** matrix one should multiply $\boldsymbol{\phi}_c$ with $-\boldsymbol{\omega^2}\ and - \boldsymbol{2\omega\zeta}$ which are given in the **A** matrix formulation. Formulation of $\boldsymbol{C}$ matrix can be shown for accelerometer type sensors as

$$\boldsymbol{C} = [-\boldsymbol{\phi}_c\boldsymbol{\omega^2} \quad -\boldsymbol{\phi}_c(\boldsymbol{2\omega\zeta})]$$

Then the result for this case is

$$\boldsymbol{C_1} = -\boldsymbol{\phi}_c\boldsymbol{\omega^2} = 1e7\begin{bmatrix} -0.0450 & 0.0073 & -0.4533 & -3.6856 & 4.4097 \\ 0.0028 & 0.2749 & 0.0860 & -3.5613 & -2.0912 \end{bmatrix}$$

$$\boldsymbol{C2} = -\boldsymbol{\phi}_c(\boldsymbol{2\omega\zeta})$$

$$= 1e3\begin{bmatrix} -0.0293 & 0.0047 & -0.2766 & -1.4481 & 1.1328 \\ 0.0018 & 0.1780 & 0.0525 & -1.3992 & -0.5372 \end{bmatrix}$$

$$\boldsymbol{C} = [\boldsymbol{C1}\ \boldsymbol{C2}]$$

D matrix

The mode shape functions necessary for $\boldsymbol{D}$ matrix calculations are already given. $\boldsymbol{D}$ matrix is mathematically defined for accelerometer sensors as

$$\boldsymbol{D} = [\boldsymbol{\phi}_s\boldsymbol{\phi}_f^T]$$

Where $\boldsymbol{\phi}_s$ is the mode shape values at the sensor locations which are given at $\boldsymbol{\phi}_c$ actually, and $\boldsymbol{\phi}_f^T$ is the mode shape values at the excitation locations which

is actually lower half of the **B** matrix. Then **D** matrix is calculated for our case as

$$D = \begin{bmatrix} -26.45 \\ 9.11 \end{bmatrix}$$

3.7   Comparison of FEA and State Space Model for Complex Structure

To verify the model state space representation of 3D structure is compared with the transient response results of NATRAN/PATRAN software. 10 modes are modelled and 5% damping is given to each mode. Then step input of 1N is applied to the given locations. Response from the same point is measured and compared. A step input is given in the Y axis. The structure is fixed from the lower side shown with filled rectangle.
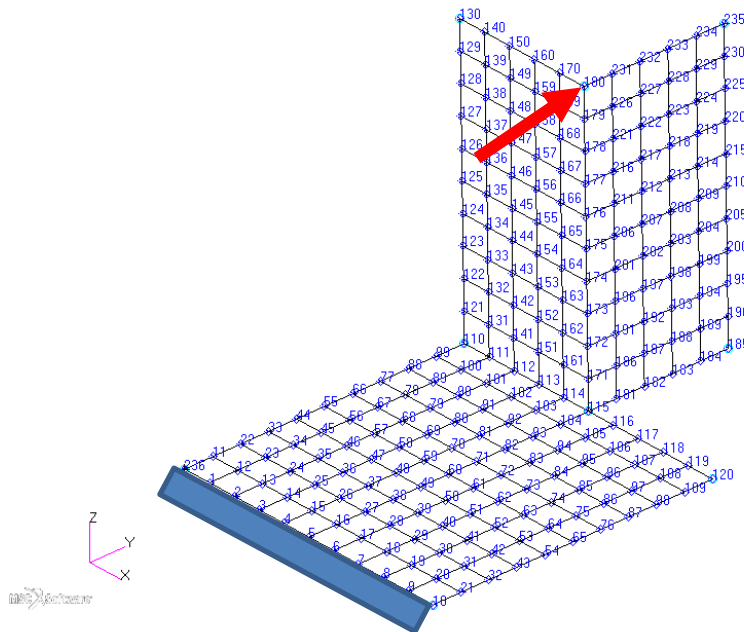
Figure 3-9 Complex Structure Step Input from Y Axis

The results and errors are drawn in the figure 10 and figure 11. It can be seen that error is around 0.1%. Also a sine input of 10Hz with 1N amplitude is given from node 235 in X axis shown in figure 12. The results and error rate can be found in the figure 13 and figure 14 respectively. Error is around 3%.
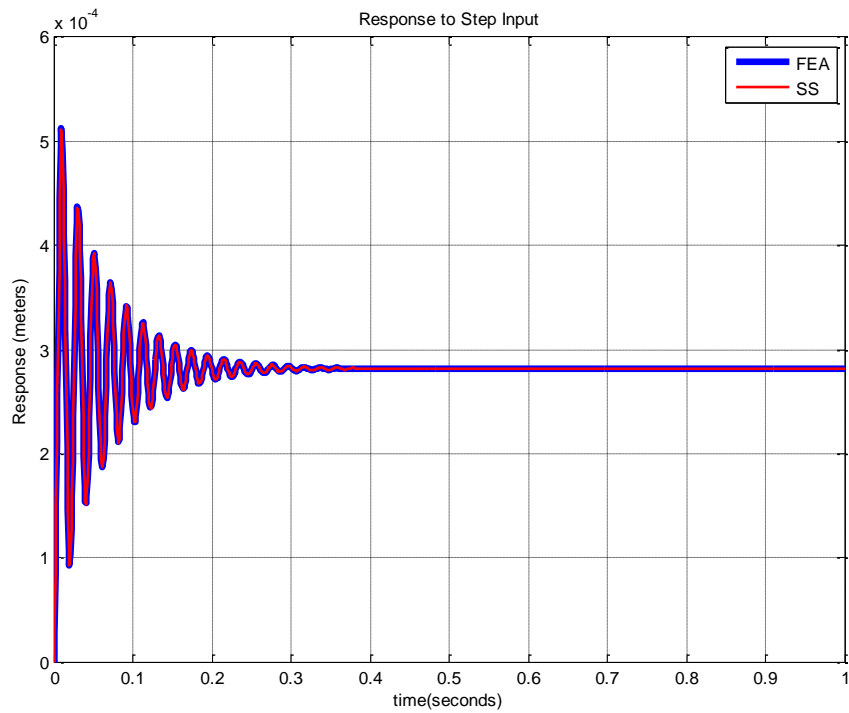
Figure 3-10 – Comparison of FEA and SS Responses to Step Input
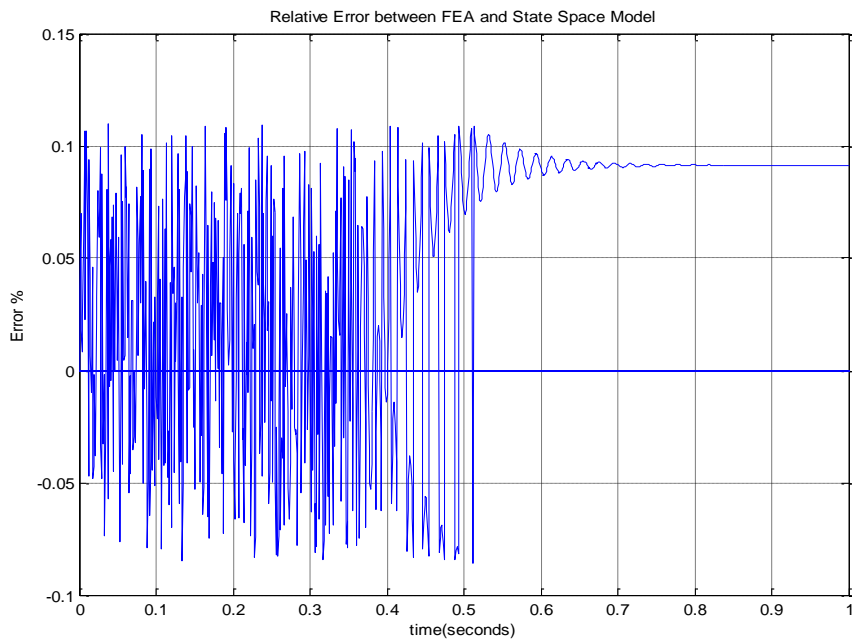
Figure 3-11 Error Percentage between FEA and SS Response to Step Input
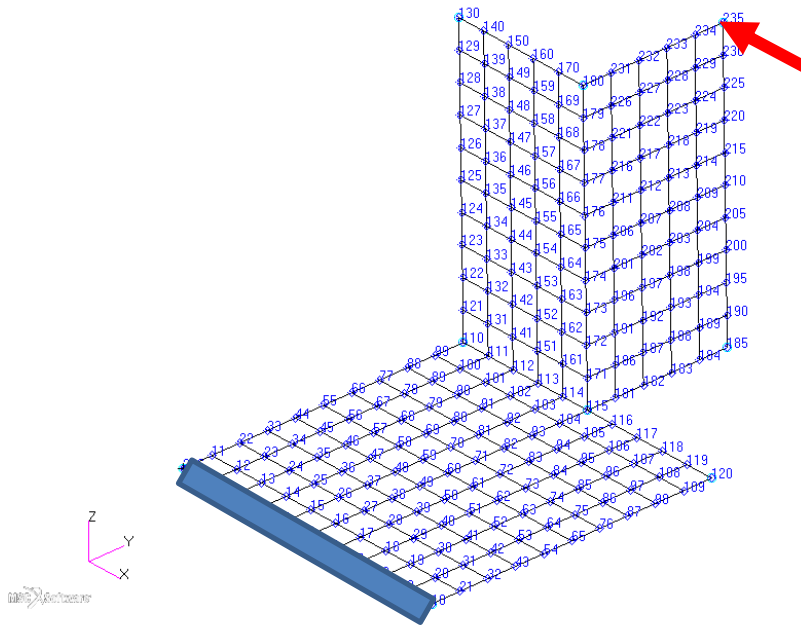
Figure 3-12 Complex Structure Sinusoidal Input from Y Axis
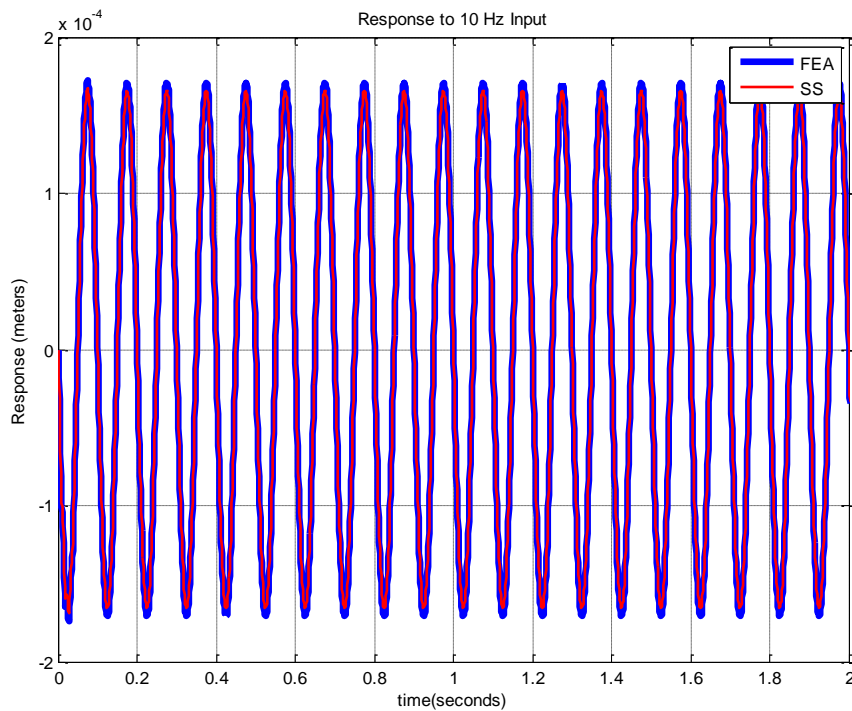
Figure 3-13 Comparison of SS and FEA Responses to Sinusoidal Disturbance
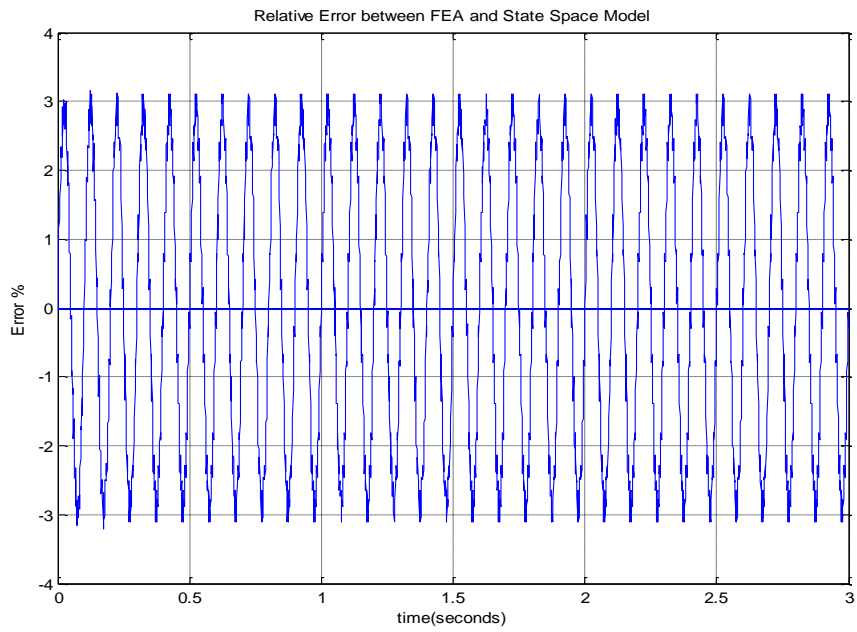
Figure 3-14 Error Percentage between FEA and SS Response to Sinusoidal Input

CHAPTER 4

MODAL SPACE CONTROL IN STATE SPACE

4.1 Introduction

Modal space control is the techniques used to control the vibrations of a structure in the modal domain. Feedback algorithms; pole placement and optimal control will be studied in this chapter. The feedback algorithm can be briefly written and shown as

$$\boldsymbol{u} = -\boldsymbol{Kx} \tag{4.1}$$
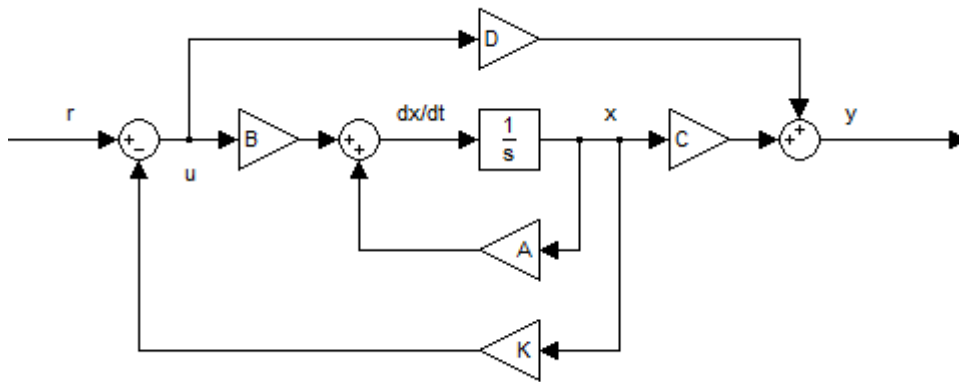
Figure 4-1 Feedback Gain Controller in State Space

Where $\boldsymbol{u}$ is the control force, $\boldsymbol{K}$ is the gain matrix and $\boldsymbol{x}$ is the state vector. Control algorithms in modal domain can be categorized into two, coupled control and independent control. In the case of independent control, control forces are obtained in modal domain as modal forces and they are only dependent on the controlled mode. If we define the modal force as $f_r(t)$ then modal force for IMSC is defined as

$$f_r(t) = -g_r \eta_r - h_r \dot{\eta}_r \tag{4.2}$$

where g_r and h_r are feedback gains, which are independently calculated for each mode.

Other cases where the modal force is also dependent on other modes is called the coupled control. The advantage of IMSC lies in the simplicity of controller design and better physical understanding of controller. Furthermore closed form solutions for pole placement and steady state optimal control are possible.

The coefficients g and h will be found separately for pole placement and optimal control. Before that, the connection between modal force and real forces will be shown. For point forces the relation between modal force and real force is

$$f(t) = B_L F(t) \tag{4.3}$$

Where B_L is the lower half of B matrix, $f(t)$ is modal force and $F(t)$ is real force. Having f number of actuators and m modes the size of the matrix B_L is (fxm). B_L does not have to be a square matrix but if that is the case a pseudo-inverse will be necessary to calculate the real forces $F(t)$.

$$F(t) = B_L^+ f(t) \tag{4.4}$$

And placing (4.2) into (4.4) K can be obtained as

$$K = B_L^+ [-G\eta(t) - H\dot{\eta}(t)] \tag{4.5}$$

Where G *and* H are diagonal gain matrices with the respective coefficients for each mode. In the above expression + is used for pseudo inverse operation. If the number of modes is equal to number of actuators (i.e. m=f) then the pseudo-inverse can be changed with the real inverse. Pseudo inverse will not generate genuine result if f<m which is a limitation for independent modal space control. It is advised that one should at least use one separate actuator for each mode. For coupled control the feedback gain matrix K is directly calculated without any transformation between modal domain and physical domain.

4.2   Controller Design

4.2.1   Pole Placement

Pole placement is a technique where the closed loop poles of the dynamic system is placed to desired locations. To be able to control a system with pole placement following criterion must be satisfied [34].

- The system is completely state controllable
- The state variables are measurable and are available for feedback.
- Control inputs are unconstrained.

The controllability criterion will be shown at the Section 4.2.4. In modal control, state variables are not physical variables but they are in the modal domain. To access the states, an observer must be used as will be discussed in Section 4.3. Control inputs will be unconstrained in the simulation environment. However

maximum values can be read from the simulation and poles can be located considering the required peak forces and limits of the actuator employed.

Modal equation will be rewritten to demonstrate the controller design

$$\ddot{\eta}_r(t) + 2\omega_r\zeta_r\dot{\eta}(t) + \omega_r^2\eta_r(t) = f_r(t), \qquad r = 1,2\ldots \tag{4.6}$$

For IMSC, to find the $\mathbf{K}$ matrix, equation (4.2) is substituted into (4.6) and all the terms are collected at one side

$$\ddot{\eta}_r(t) + (2\omega_r\zeta_r + h_s))\dot{\eta}(t) + (\omega_r^2 + g_s)\eta_r(t) = 0,$$
$$r = 1,2\ldots \tag{4.7}$$

Assume that it is required to place the poles of rth mode at $-a_r + i\beta_r$ then the response of the mode can be written as

$$\eta_r(t) = c_r e^{(-a_r + i\beta_r)t} \tag{4.8}$$

Place equation (4.8) into (4.7) to find the g_r and h_r.as

$$g_r = a_r^2 + \beta_r^2 - w_r^2 \tag{4.9}$$

$$h_r = 2a_r - 2\omega_r\zeta_r \tag{4.10}$$

α, β are shown in the figure 4-2. α is the real part and β is the imaginary part of the pole which are defined by equations (4.11.-4.12) respectively and shown in the figure (4.2)

$$\alpha_r = -\zeta_{r_{desired}}w_r \tag{4.11}$$

$$\beta_r = w_r\sqrt{1 - \zeta_{r_{desired}}^2} \tag{4.12}$$
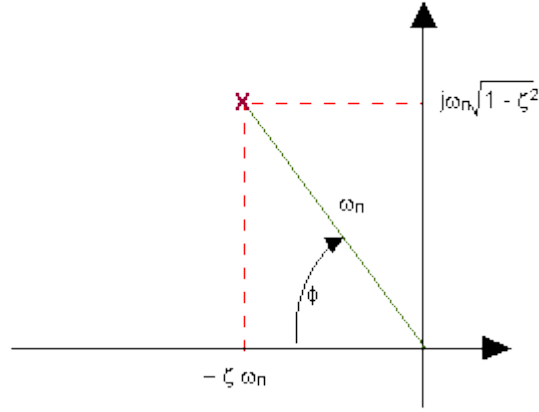
Figure 4-2 Placement of Poles [35]

It is not necessary to change the natural frequency of the system for most cases, therefore β_r should be equal to ω_r then g_r and h_r can be defined as

$$g_r = \alpha_r^2 = \zeta_{r_{desired}}^2 \omega_r^2 \tag{4.13}$$

$$h_r = 2\omega_r(\zeta_{r_{desired}} - \zeta_r) \tag{4.14}$$

From g_r, h_r and locations of actuators one can calculate the real forces to place the poles of the system at required positions.

For coupled control a closed form solution is not available. One needs to solve the characteristic equation. Characteristic equation for open loop system can be written as

$$det|sI - A| = (s - \mu_1)(s - \mu_2)\dots(s - \mu_3) \tag{4.15}$$

Where $\mu_1, \mu_2, \dots, \mu_m$ are the open loop poles of the system. Then considering feedback matrix K, closed loop characteristic equation can be written as

$$det\,|sI - (A - BK)| = (s - \lambda_1)(s - \lambda_2)\dots(s - \lambda_m) \tag{4.16}$$

Where A and B are state space matrices and $\lambda_1 \dots \lambda_m$ are the pre-defined poles of the system. One should solve (4.16) to find the feedback gain values.

4.2.2   Optimal Control

Despite the fact that poles can be located at any arbitrary point with pole location technique, it does not guarantee the optimal solution for control. Optimal control

50

suggest a solution such that there is a special $u^*(t)$ control function which minimizes the cost function comparing with any other $u(t)$. Minimization of cost function maximizes the performance. The cost function can be chosen for minimum time such as

$$J = t_f - t_0 = \int_{t_0}^{t_f} dt \tag{4.17}$$

Another option for cost function is called linear regulator problem. The aim is to return the states of the system to 0. It is defined as

$$J = \frac{1}{2} \int_{t_0}^{t_f} (x^T Q x + u^T R u) dt \tag{4.18}$$

Where Q and R are positive definite symmetric weighting matrices. The regulator type cost function is appropriate for vibration suppression applications. Then continuing with the regulator problem, Q can be selected such that $x^T Q x$ defines the total energy in the system. If states are defined in the form

$$x = [\eta \; \dot{\eta}]^T \tag{4.19}$$

Then Q matrix can be written as

$$Q = \frac{1}{2} \begin{bmatrix} \omega^2 & 0 \\ 0 & I \end{bmatrix} \tag{4.20}$$

The R matrix should be chosen by the designer. Increasing the value of R puts more importance to controller which reduces the force values. If there is a limit for force values then designer should find a R matrix iteratively such that maximum $u(t)$ is lower than the available peak force. R can be chosen such that different importance can be given to different actuators. As R value increases importance of force or energy supplied to the system increases, therefore more oscillations are seen. On the other hand when R value decreases, oscillations attenuate quickly but peak force is increased.

The feedback matrix K can be found by

$$K = R^{-1} B^T P(t) \tag{4.21}$$

51

And $P(t)$ is found by solving the matrix Riccati Equation

$$A^T P(t) + P(t)A - P(t)BR^{-1}B^T P(t) + Q = -\dot{P}(t) \qquad (4.22)$$

Solving the matrix Riccati Equation requires the solution of 2m(2m+1)/2 non-linear ordinary differential equations. If one only interested for steady state response then t_f is assumed to be infinity and for steady state $\dot{P}(t)$ term vanishes. The matrix Riccati Equation is now a nonlinear algebraic equation.

If one considers the independent modal space scheme for optimal control then the number of modes for each case reduces to 1 and $P(t)$ becomes a 2x2 matrix. In this case it is required to solve three nonlinear ordinary DE for each mode independently. For IMSC, the definition of x and A, B for f number of point actuators on the structure at points $x_1, x_2, \ldots, x_f$ at r^{th} mode can be written as

$$x_r = [\eta_r \; \dot{\eta}_r]^T{}_{2x1} \qquad (4.23)$$

$$A_r = \begin{bmatrix} 0 & 1 \\ -\omega_r^2 & -2\omega_r\zeta_r \end{bmatrix}_{2x2} \qquad (4.24)$$

$$B_r = \begin{bmatrix} 0 & 0 & \ldots & 0 \\ \phi_r(x_1) & \phi_r(x_2) & \ldots & \phi_r(x_f) \end{bmatrix}_{2xf} \qquad (4.25)$$

If it is necessary to optimize the problem for steady state case, then the solution of the optimal control problem is given by Meirovitch [9] as

$$g_r = -\omega_r^2 + \omega_r(\omega_r^2 + R_r^{-1})^{\frac{1}{2}} \qquad (4.26)$$

$$h_r = -2\zeta_r\omega_r + \left[4\zeta_r^2\omega_r^2 + R_r^{-1} - 2\omega_r^2 + 2\omega_r(\omega_r^2 + R_r^{-1})^{\frac{1}{2}}\right]^{\frac{1}{2}} \qquad (4.27)$$

For coupled control one should solve the Riccati Algebraic Equation system with 2m(2m+1)/2 equations. Then K matrix can be obtained directly from the solution.

4.2.3 Controllability

Controllability is defined as ability to move a state of the system from one any initial condition to a defined state in a finite time interval. The controllability matrix is defined as

$$C = [B\ AB\ A^2B\ ... A^{2m-1}B] \qquad (4.28)$$

And if the **C** matrix has the rank 2m then the system is deemed as controllable.
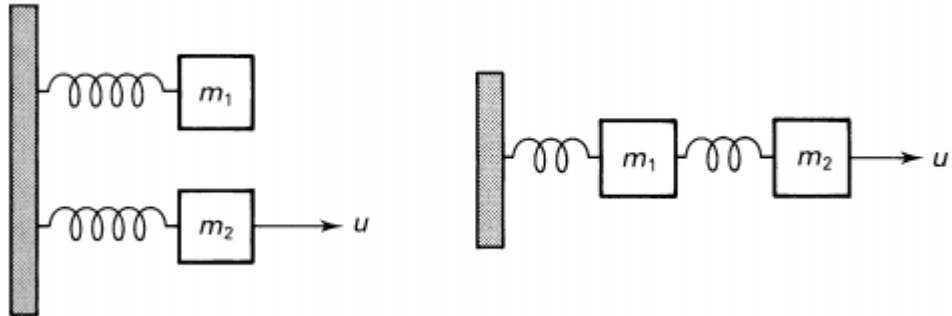
Figure 4-3 Uncontrollable and Controllable Systems [32]

Figure 4-3 shows uncontrollable and controllable system examples.

4.3   Observer Design

4.3.1   Introduction

Modal space control requires the modal displacement and velocity values to calculate the necessary control input for the structure. However, it is not possible to measure the modal coordinates physically. Therefore, either by using displacement, velocity and acceleration measurements the modal states must be estimated by using an observer.

Kalman has proposed an optimal observer that contains measurement and actuator noise [36]. Luenberger has summed up observers for systems without noise [37]. Luenberger observer is selected for the simulations in this study due to its simplicity.

Placing the sensors to arbitrary nodes are not enough to find all the states. They must be located such that observability matrix has full rank. Then, all the states can be obtained and the selected control algorithm can be used.

4.3.2   Observability

Observability can be defined as the ability to obtain the every state of the plant in finite time by using only the outputs of the system. The observability is based on the rank of the matrix given below

$$O = \begin{bmatrix} C \\ CA \\ CA^2 \\ \dots \\ CA^{2m-1} \end{bmatrix} \qquad (4.29)$$

If rank of O equals to 2m, it is said that the plant is observable for our case.

4.3.3 Observer Design

The state space form of the plant is rewritten as

$$\dot{x} = Ax + Bu \qquad (4.30)$$

$$y = Cx + Du \qquad (4.31)$$

Then an observer is designed to estimate the values of states and correcting itself with the outputs taken from the exact system. The ~ mark is used to distinguish observer from plant. K_e is the observer feedback gain. The observer dynamics can be written as

$$(\dot{\tilde{x}}) = A\tilde{x} + Bu + K_e[y - (C\tilde{x} + Du)] \qquad (4.32)$$

$$(\dot{\tilde{x}}) = A\tilde{x} + Bu + K_e y - K_e C\tilde{x} - K_e Du \qquad (4.33)$$

Error is defined as the difference between the real states and estimated states shown in the equation below

$$e = x - (\hat{x}) \qquad (4.34)$$

Putting equation (4.31) into (4.33), and subtracting (4.33 from (4.30)

$$-[(\dot{\tilde{x}}) = A\tilde{x} + Bu + K_e Cx + K_e Du - K_e C\tilde{x} - K_e Du] \qquad (4.35)$$

$$+\dot{x} = Ax + Bu \qquad (4.36)$$

Will give the error rate between states.

$$\dot{x} - (\dot{\tilde{x}}) = A(x - \tilde{x}) - K_e C(x - \tilde{x}) \qquad (4.37)$$

$$\dot{e} = (A - K_e C)e \qquad (4.38)$$

K_e is selected such that the poles of the observer are five to ten times larger than the actual system. Observer model is shown in the figure below.
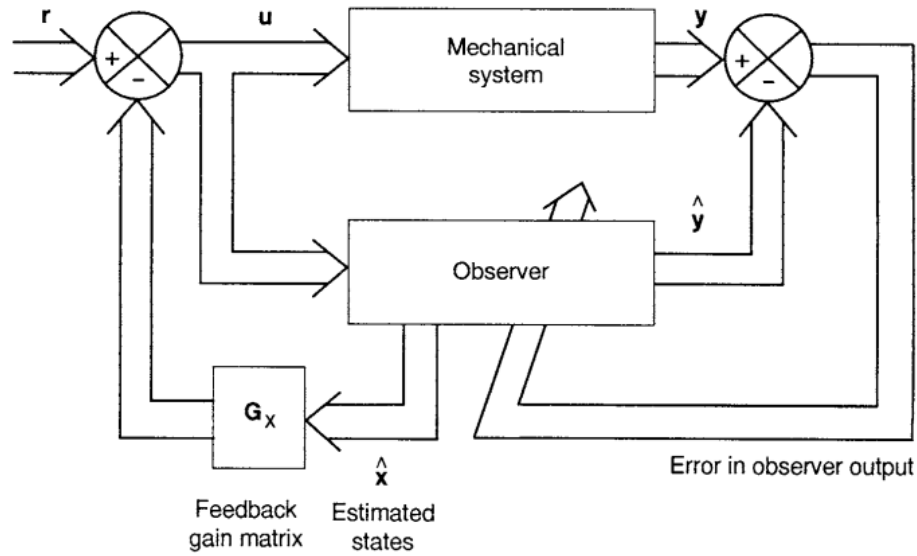
Figure 4-4 Observer and Plant [38]

4.4 Controlling Selected Modes

It is not always necessary to control all modelled modes of the structure. Then one should modify the previous equations to control the selected modes of the system. If m is the total number of modelled modes, it can be divided as m_c and m_r, number of controlled modes and number of residual modes respectively. Also the states can be re-written as

$$x = [\boldsymbol{\eta}_c \; \dot{\boldsymbol{\eta}}_c \; \boldsymbol{\eta}_r \; \dot{\boldsymbol{\eta}}_r]^T$$

where $\boldsymbol{\eta}_c$ is the controlled mode vector and $\boldsymbol{\eta}_r$ is the residual mode vector. With the new states $\boldsymbol{A}$ and $\boldsymbol{B}$ matrices is required to be redefined. $\boldsymbol{A}$ matrix is separated into $\boldsymbol{A}_c$ and $\boldsymbol{A}_r$ matrices with the same structure of the original $\boldsymbol{A}$ matrix. However they only contain their respective modes. It can be formulated as

$$A = \begin{bmatrix} A_c & 0 \\ 0 & A_r \end{bmatrix}$$

$$B = \begin{bmatrix} B_c \\ B_r \end{bmatrix}$$

Where A_c is $2m_c \times 2m_c$ and A_r is $2m_r \times 2m_r$ sized matrix. B_c matrix only contains the mode shape values of controlled modes and B_r contains the mode shape values of residual modes.

One should also redefine the C matrix to adapt the changed state vector.

$$C = [C_c \ C_r]$$

Where C_c is for controlled modes and C_r for residual modes. D matrix remains unchanged.

The controller and estimator equations also require modification. Less number of modes are controlled therefore less number of modes are necessary for estimation. Now the controller defined in equation (4.1) is changed into

$$u = -Kx_c$$

To find the controller gain K, same algorithms are used however instead of A and B, A_c and B_c matrices are used. One can see that u vector is multiplied by both B_c and B_r. The controlled modes are contributing to the control of the system. On the other hand residual modes are also contributing to the system response and create unwanted oscillations. This is called **control spillover**. Meirovitch stated that control spillover reduces the system performance but does not destabilize the system.

Observer is modified such a way that only the modal states that are needed for the controlled modes are estimated. Residual modes are not estimated therefore their effect cannot be put into the observer equation. Then equations (4.32) can be written as

$$\dot{\tilde{x}}_c = A_c\tilde{x}_c + B_c u + K_e[y - (C_c\tilde{x}_c + Du)] \qquad (4.39)$$

However in the real case the output is sum of both controlled modes and residual modes. Modes that are not contributed into the observer create an error and it is called **observation spillover.** Meirovitch stated that observation spillover can destabilize the system. To overcome the problem it is stated that active vibration control is mostly used on lower modes and upper modes are selected as residual modes. One can filter out the higher frequencies to prevent observer spillover.

CHAPTER 5

CASE STUDIES

5.1   Introduction

In this chapter case studies will be demonstrated. Two models will be used; simply supported beam with transverse vibrations and a three dimensional complex shape shown in Chapter 3 with three translational degrees of freedom at each node.

Number of controlled modes, location of sensors, actuators and disturbances are changed to show the applicability of control algorithms. For applicable conditions independent modal space control and coupled control is shown. For other cases only coupled control is used.

Matlab and Simulink are used to simulate the models. Response of the each controller and controller force is compared with each other. For optimal control different R (weight of the actuator) is used.

5.2   Simply Supported Beam

5.2.1   Model Definition

A simply supported beam shown in Chapter 3 is used in the case study. Its properties are shown in Table 5.1

Table 5-1 Simply Supported Beam Properties

Length	1000 mm
Width	100 mm
Height	10 mm
Young's Modulus of Elasticity	70 Gpa
Density	2700 kg/m^3
Boundary Conditions	Pinned from both ends
Number of Nodes	21
Number of modelled Modes	6

It was shown that the results of the finite element model results are in good agreement the analytical case. Actually, error of natural frequencies and mode shapes are less than 1% for the first six modes. First six natural frequencies are shown in Table 5.2.

Table 5-2 Simply Supported Beam Natural Frequencies

1st Mode	2nd Mode	3rd Mode	4th Mode	5th Mode	6th Mode
23.086 Hz	92.306 Hz	207.550 Hz	368.600 Hz	575.120 Hz	826.570 Hz

The mode shape matrix is given in Table 5.3. It is necessary to display it here to show how to locate the sensors and actuators. The numbering of nodes are shown in Figure 5.1.

Table 5-3 Mode Shapes Matrix of the Simply Supported Beam

Node	1st Mode	2nd Mode	3rd Mode	4th Mode	5th Mode	6th Mode
1	0	0	0	0	0	0
2	-0.134637	0.265959	-0.39073	-0.50589	0.608581	0.696291
3	-0.265959	0.505885	-0.69629	-0.81854	0.860663	0.818539
4	-0.390733	0.696291	-0.85007	-0.81854	0.608581	0.265959
5	-0.505885	0.818539	-0.81854	-0.50589	0	-0.50589
6	-0.608581	0.860663	-0.60858	0	-0.60858	-0.86066
7	-0.696291	0.818539	-0.26596	0.505885	-0.86066	-0.50589
8	-0.766856	0.696291	0.134637	0.818539	-0.60858	0.265959
9	-0.818539	0.505885	0.505885	0.818539	0	0.818539
10	-0.850067	0.26596	0.766856	0.505885	0.608581	0.696291
11	-0.860663	0	0.860663	0	0.860663	0
12	-0.850067	-0.26596	0.766856	-0.50589	0.608581	-0.69629
13	-0.818539	-0.50589	0.505885	-0.81854	0	-0.81854
14	-0.766856	-0.69629	0.134638	-0.81854	-0.60858	-0.26596
15	-0.696291	-0.81854	-0.26596	-0.50589	-0.86066	0.505885
16	-0.608581	-0.86066	-0.60858	0	-0.60858	0.860663
17	-0.505885	-0.81854	-0.81854	0.505885	0	0.505885
18	-0.390733	-0.69629	-0.85007	0.818539	0.608581	-0.26596
19	-0.26596	-0.50589	-0.69629	0.818539	0.860663	-0.81854
20	-0.134637	-0.26596	-0.39073	0.505885	0.608581	-0.69629
21	0	0	0	0	0	0
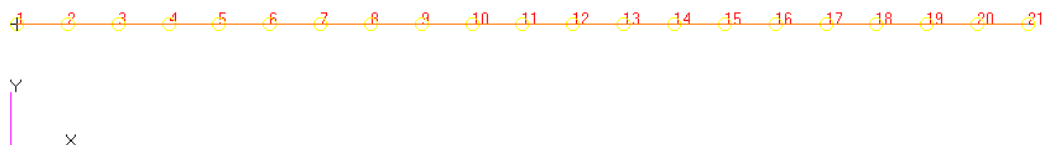
Figure 5-1 Node Numbers of Simply Supported Beam

Beam is vibrating in the Y direction and pinned at the nodes 1 and 21.

5.2.2 Case Studies

5.2.2.1 First Mode Control

In this case study only first mode will be controlled with one sensor and one actuator and one disturbance force. Step input and a sinusoidal input will be given to the system. Force response function will be obtained for selected cases. 1% damping is introduced into the model for each mode. As the number of actuator is equal to the number of controlled mode, independent modal space control is applicable in this case. The aim is to re-locate the damping of first mode to $1/\sqrt{2}$.

For the first sub-case, disturbance will be put at 6th node with 1 Newton amplitude, displacement sensor at 10th node and actuator at 11th node. Also R is taken as 0.001. Then for step input the results are shown in the figure 5.2. The required force for each case is given in the figures 5.3
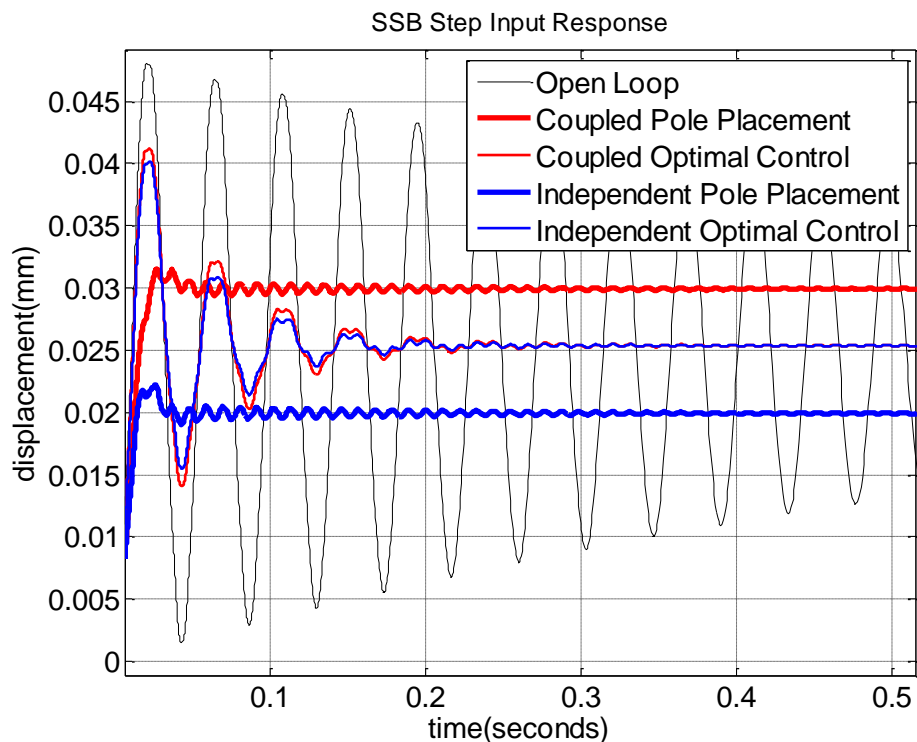
Figure 5-2 Simply Supported Beam Response to Step Input
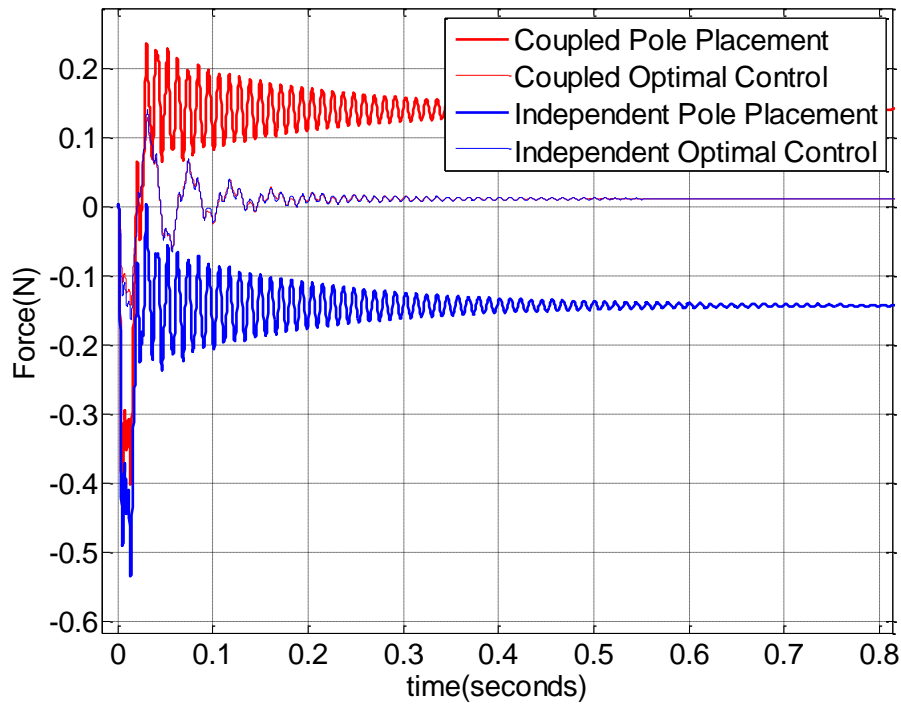
Figure 5-3 Simply Supported Beam Force Comparison to Step Response Disturbance

The response to step input is satisfactory such that vibrations are reduced in less than 0.05 seconds for pole placement case. For optimal control different R values are compared in the Figure 5.4. In the figure 5.5 force required to control the system is shown. To compare them easily, their absolute value is taken. One can select an appropriate R value for the available maximum force output of the actuator.
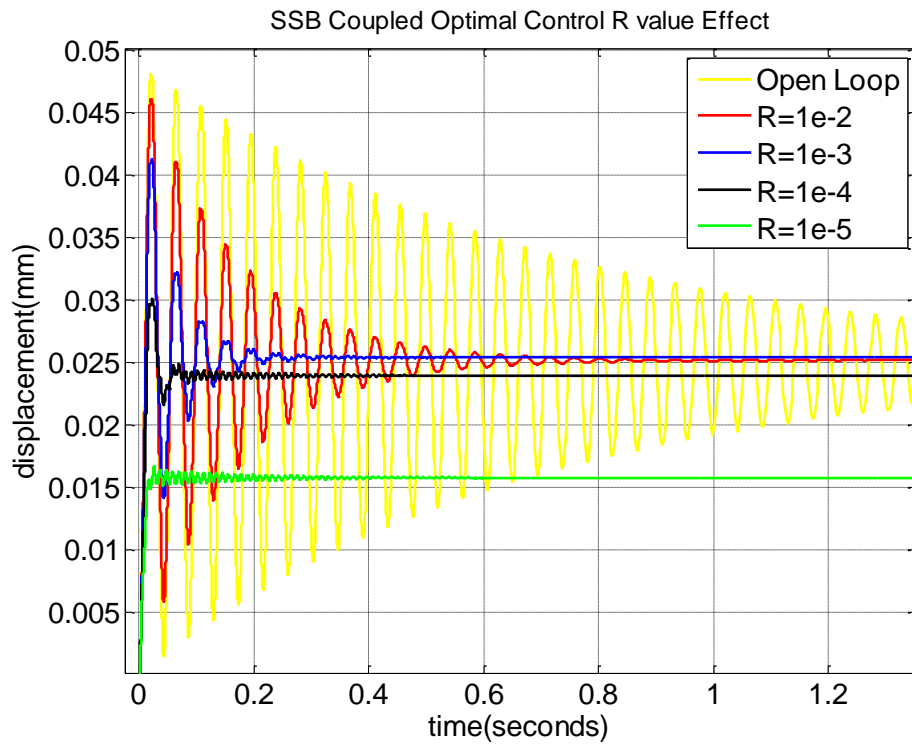
Figure 5-4 SSB Step Response Coupled Optimal Control for Different R values (displacement)
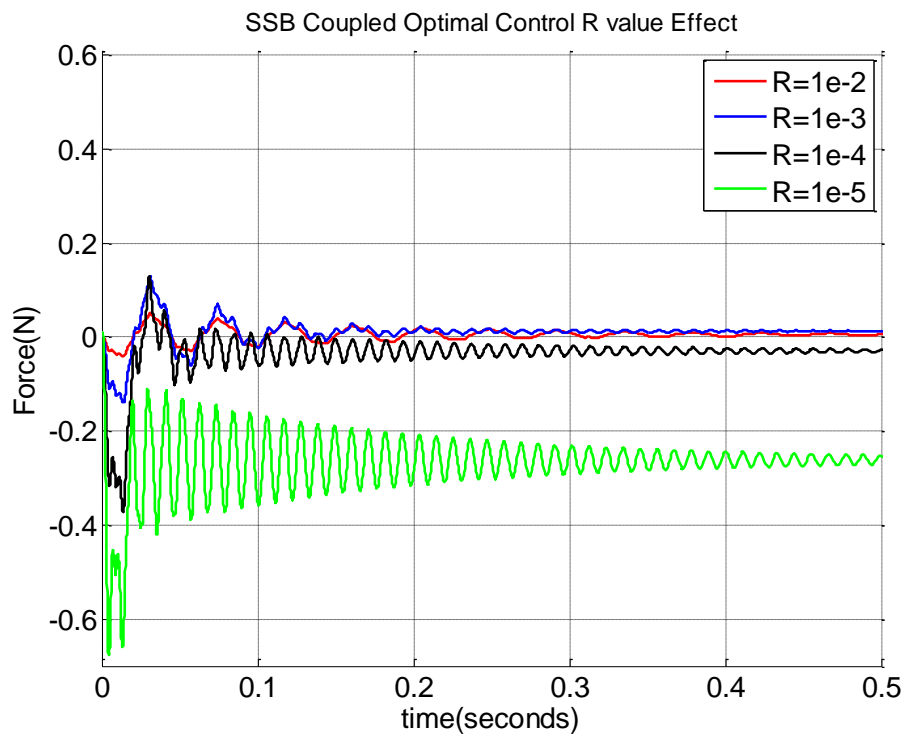
Figure 5-5 SSB Step Response Coupled Optimal Control for Different R values (Force)
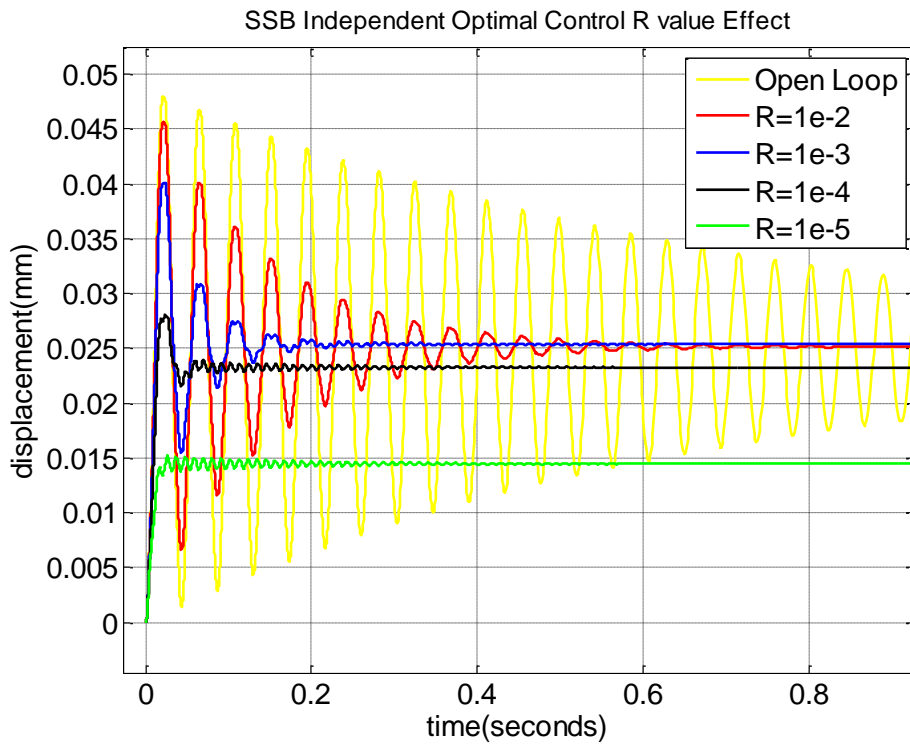
Figure 5-6 SSB Step Response Independent Optimal Control for Different R values (displacement)
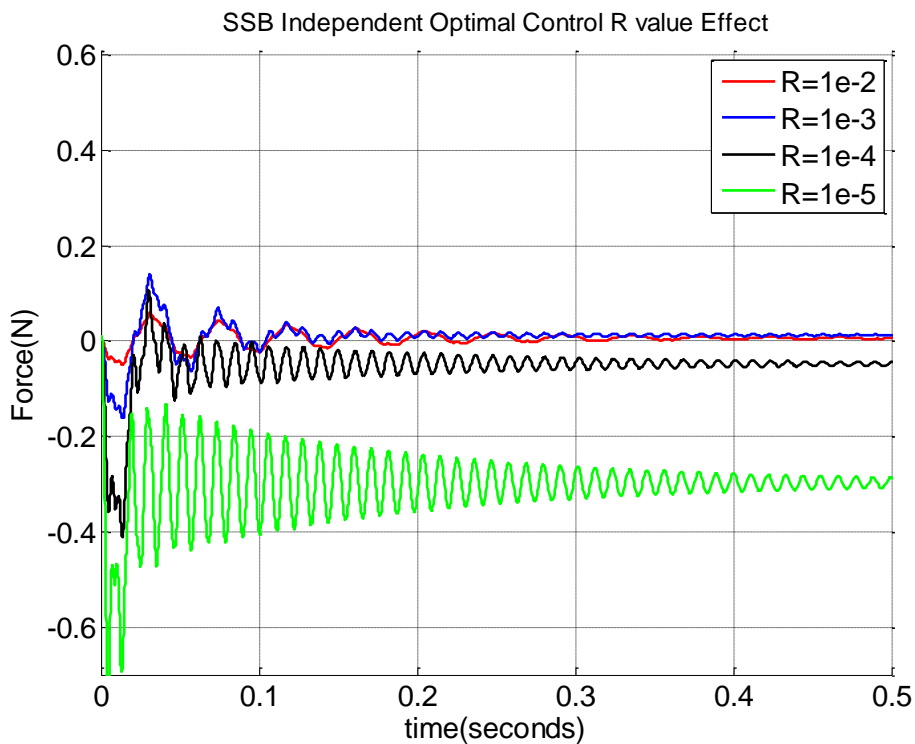
Figure 5-7 SSB Step Response Independent Optimal Control for Different R values (displacement)

It is seen that as R increases the required force decreases, however in the same time the oscillations continue longer.

Now the response of the system to sinusoidal input will be shown. A chirp signal from 2 Hz to 100 Hz is given in 100 seconds. In Simulink ode8 is used as fixed time step solver. Time step is given as 1/10000 seconds. Then Fast Fourier Transform(FFT) is made in Matlab. The Matlab Code for FFT is given in Appendix A The results are shown in figure 5.8.

It is seen that there is more than 20 dB decrease at the first mode for optimal control(R=0.001) and more than 30 dB decrease for pole placement. As we only control the first mode there is no change at the second mode response at the frequency around 92 Hz.
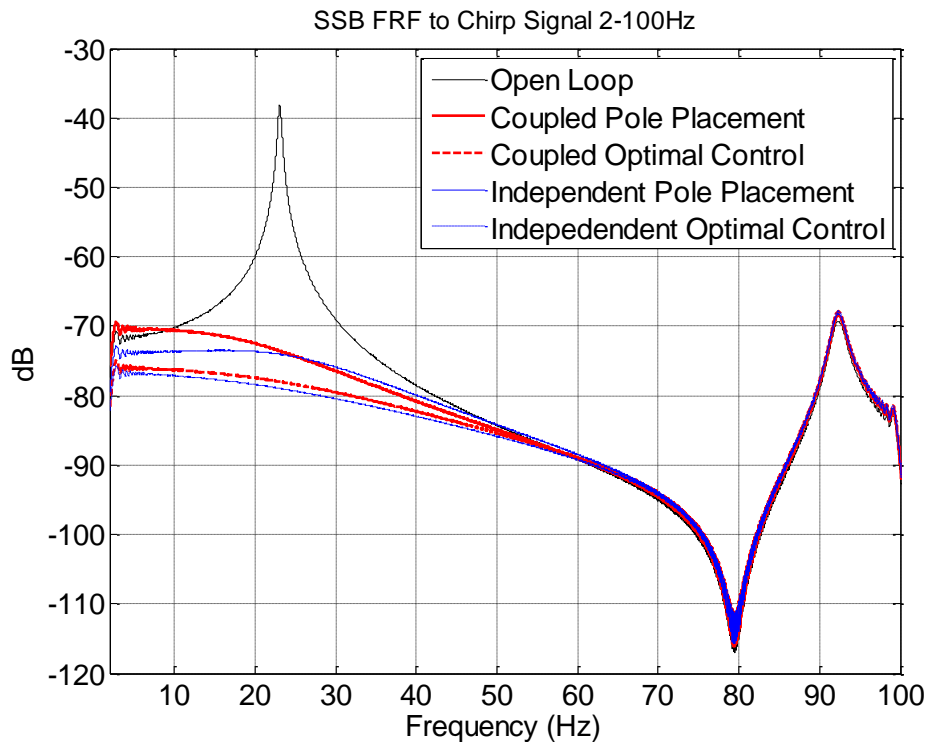
Figure 5-8 Simply Supported Beam, Frequency Response Function between 0-100 Hz, One Mode Control

5.2.2.2 *First and Second Mode Control*

In the previous sub-case it is shown that first mode is controlled. If it is necessary to control the second mode also, we need to increase the number of controlled modes to 2. In the simulation it is seen that another sensor is necessary to obtain convergence. It is probably due to observation spillover. Then the sensor

position is changed from 10th node to 7th and 14th node. Also from the mode shape matrix, table 5.3, it can be seen that actuator at 11th node has zero effect on second mode. Therefore it is re-located to the 14th node. Then same chirp signal is given to obtain the frequency response function of the model. The response of the sensor at 7th node is shown in figure 5.9 and response of sensor at 14th node is shown in figure 5.10.
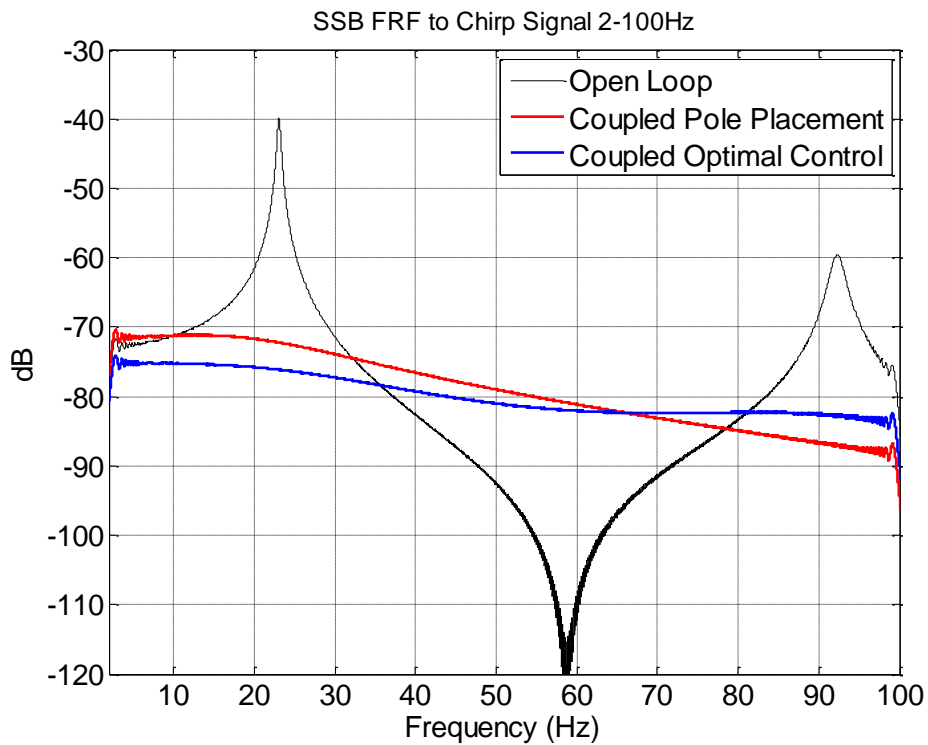
Figure 5-9 Simply Supported Beam, Frequency Response Function between 0-100 Hz, Two Mode Control, Sensor at 7th Node.

At resonances there is more than 30 dB decrease in vibrations. However in the 7th node the vibrations are increased between two resonances. At 14th node there is small increase between two resonances. The big increase at 7th node is because there is an anti-resonance located between.

64
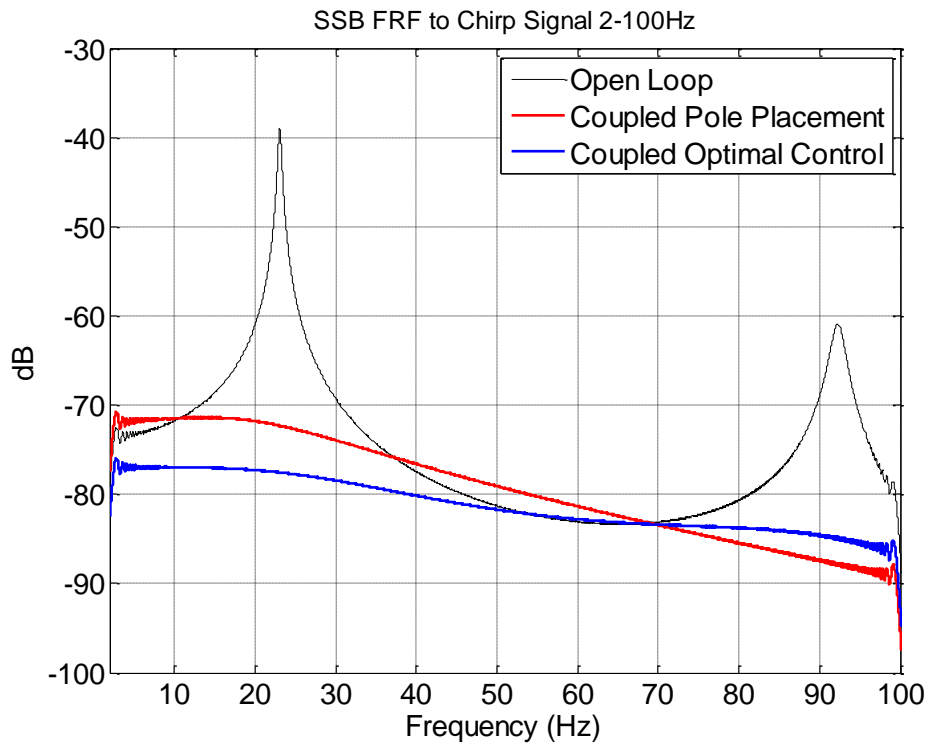
Figure 5-10 Simply Supported Beam, Frequency Response Function between 0-100 Hz, Two Mode Control, Sensor at 14th Node.

5.3 Complex Structure

5.3.1 Model Definition

A three dimensional structure with arbitrary shape is modelled in Patran and solved with Nastran. The meaning of arbitrary shape is that the structure has a feature in every plane and hence modes are not separated from each other in x, y, and z axes. The shape with node numbers is shown in Figure 5.11. Properties of the structure are given below in Table 5.4.

Table 5-4 Properties of Complex Structure

Long Sides	100 mm
Short Sides	50 mm
Thickness	2 mm
Young's Modulus of Elasticity	70 Gpa
Density	2700 kg/m^3
Boundary Conditions	Fixed from 236th and 1st -10th nodes
Number of Nodes	236
Number of modelled Modes	10
Number of DOF at each node	3 translational, X,Y,Z axis

65
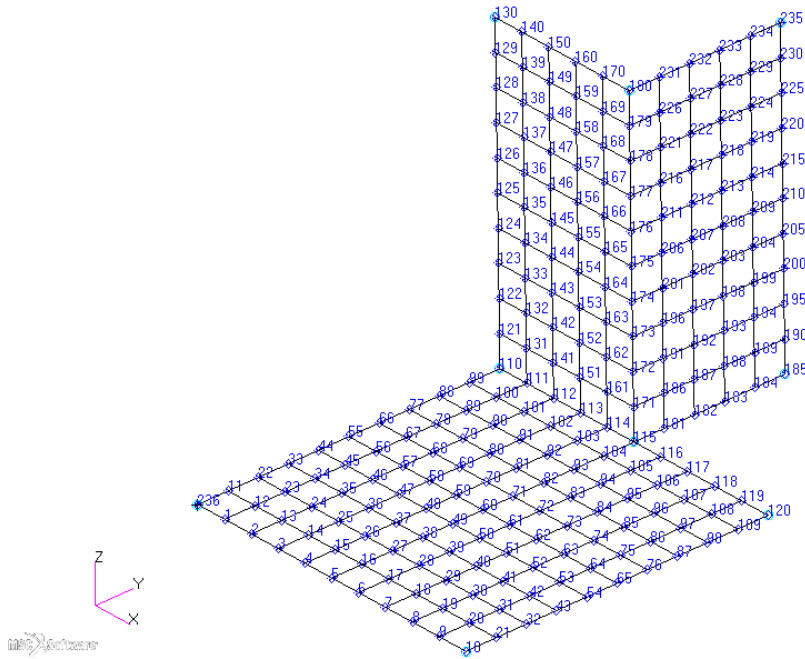
Figure 5-11 Complex Structure with Finite Element Node Numbers

It is modelled with 10 modes, 236 nodes and three translational degrees of freedom at each node. The 10 mode shapes and natural frequencies are shown in Table 5.5.

Table 5-5 Complex Structure First Ten Mode Shapes and Natural Frequencies

66
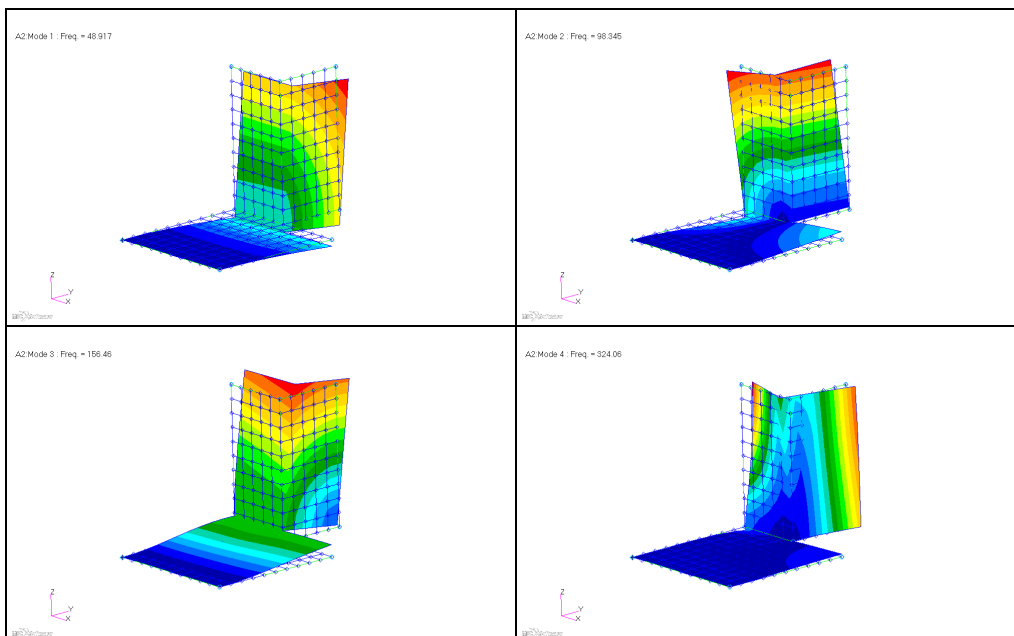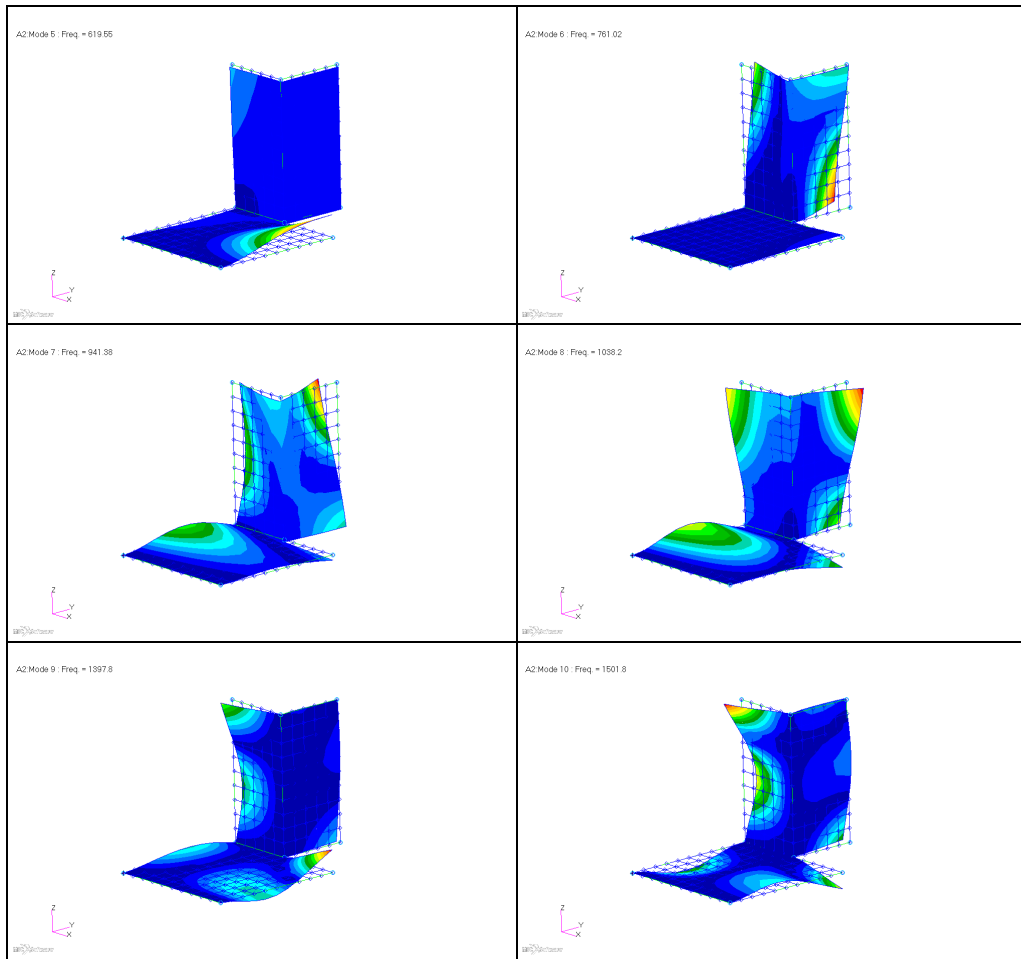
5.3.2 Case Studies

At first, 1st mode shape will be controlled. Secondly 1st and 2nd mode shapes will be controlled. In the third case only 5th mode shape will be controlled to show that higher local modes can be controlled with modal control approach.

5.3.2.1 First Mode Control

From Table 5.5 it can be seen that at first mode the structure is vibrating in ZY plane (around X axis). It is seen that there is displacement in both Y direction and Z direction. Therefore sensor and actuator can be put in those directions. A disturbance will be put such that it has a significant effect on 1st mode. For different locations and directions of sensor, actuator and disturbance, the resultant open loop and closed loop responses are shown.

i) From table 5.5 it can be seen that most displacement on first mode is at the node 235. Then sensor and actuator is co-placed at that point. Disturbance is

67

given at the node 130, which also have an effect on first mode. Ode23t solver with 0.5 simulation time is used. R value for optimal control is taken as 0.001. The results are shown in the figure 5.12.

Sensor Location - Axis	Actuator Location - Axis	Disturbance Location - Axis
235th node Z axis	235th node Z axis	130th node Z axis
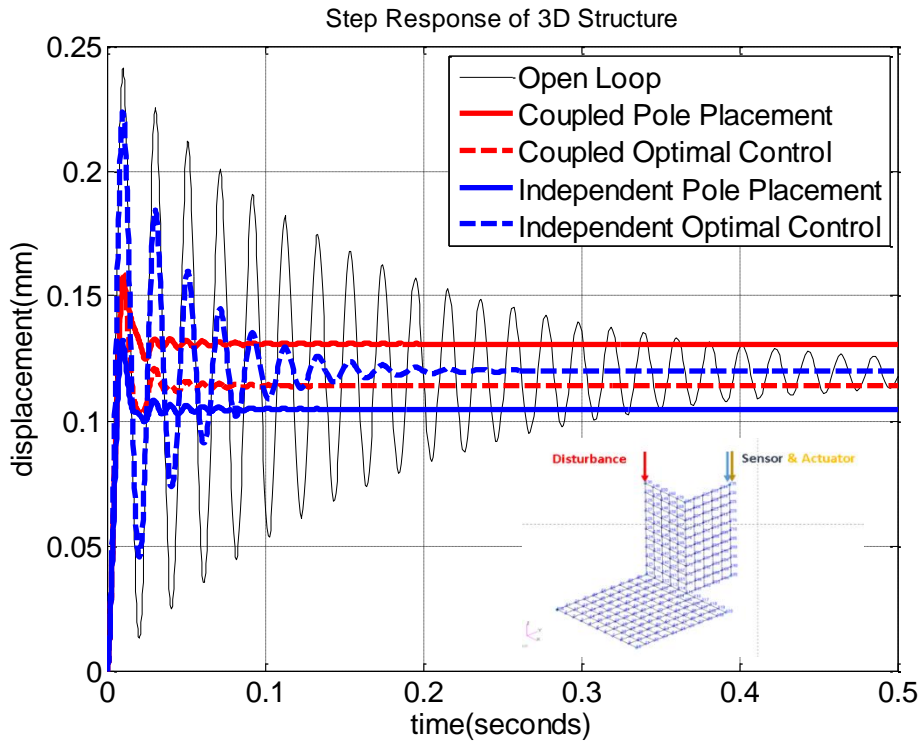
Figure 5-12 Complex Structure response to Step Input. Sensor Z axis, Actuator Z axis, Co-placed.

ii) In this case sensor direction is changed from Z axis to Y axis. The actuator and sensor are still co-placed. The result is shown in the figure 5.13

Sensor Location - Axis	Actuator Location - Axis	Disturbance Location - Axis
235th node Y axis	235th node Z axis	130th node Z axis
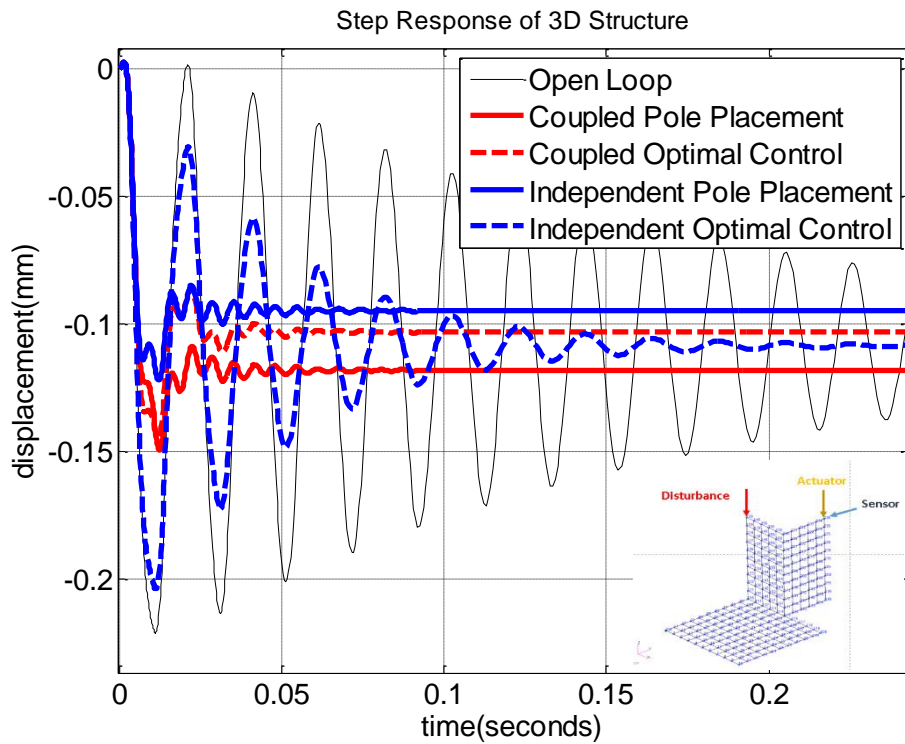
Figure 5-13 Complex Structure response to Step Input. Sensor Y axis, Actuator Z axis, Co-placed

iii) Sensor is relocated such that it is now sensing the Z axis displacement from the node 170. The results are shown in the Figure 5.14

Sensor Location - Axis	Actuator Location - Axis	Disturbance Location - Axis
170th node Z axis	235th node Z axis	130th node Z axis
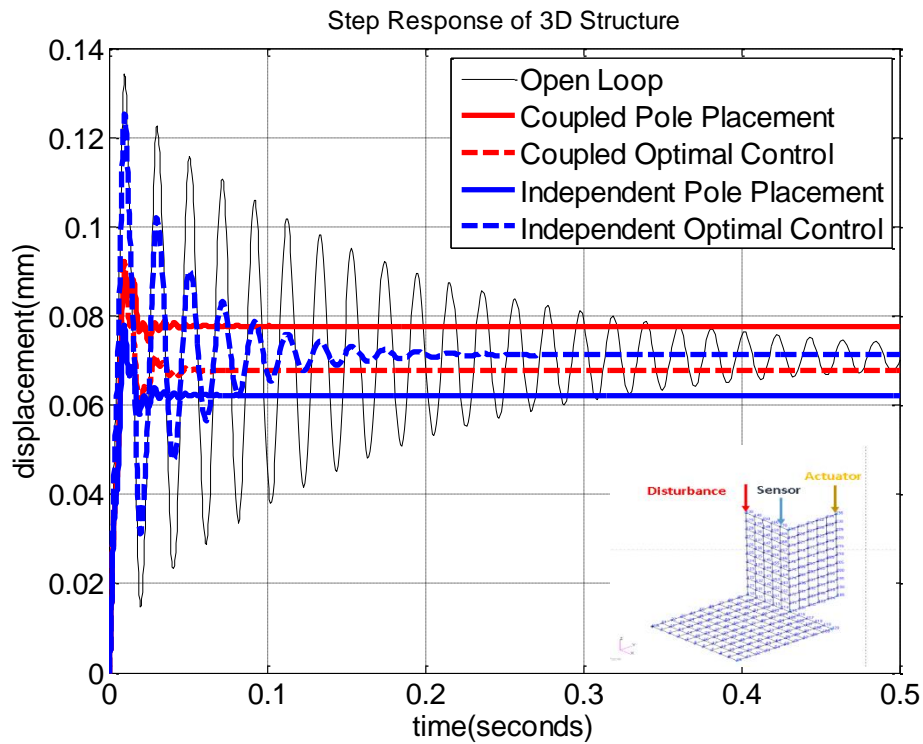
Figure 5-14 Complex Structure response to Step Input. Sensor Z axis, Actuator Z axis, Not Co-placed

iv) In the fourth case the sensor is placed such that it is not co-placed and senses the displacement in Y axis. The results are shown in Figure 5.15.

Sensor Location - Axis	Actuator Location - Axis	Disturbance Location - Axis
170th node Y axis	235th node Z axis	130th node Z axis
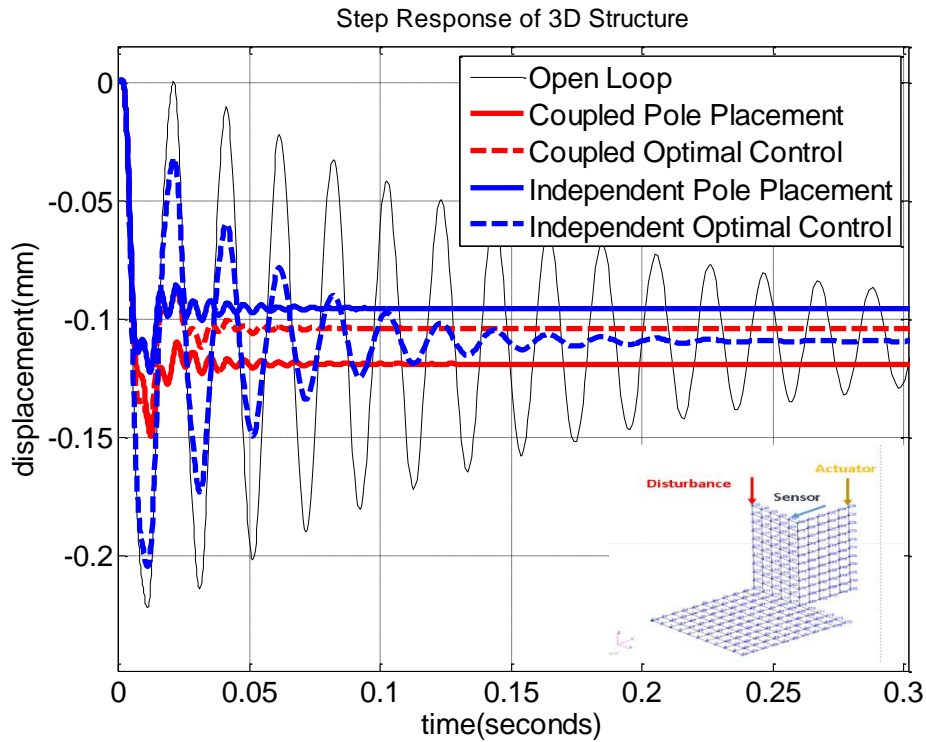
Figure 5-15 Complex Structure response to Step Input. Sensor Y axis, Actuator Z axis, Not Co-placed

v) In the fifth case frequency response function will be shown for not co-placed, different axis sensor/actuator placement case. (i.e. case iv). First two natural frequencies are 48 and 98 Hz respectively. A chirp signal from 2 Hz to 100 Hz in 100 seconds is given. The results are shown in Figure 5.16.Fixed time step solver ode8 is used with 1/10000 seconds step size. FFT is calculated with the code in Appendix A.
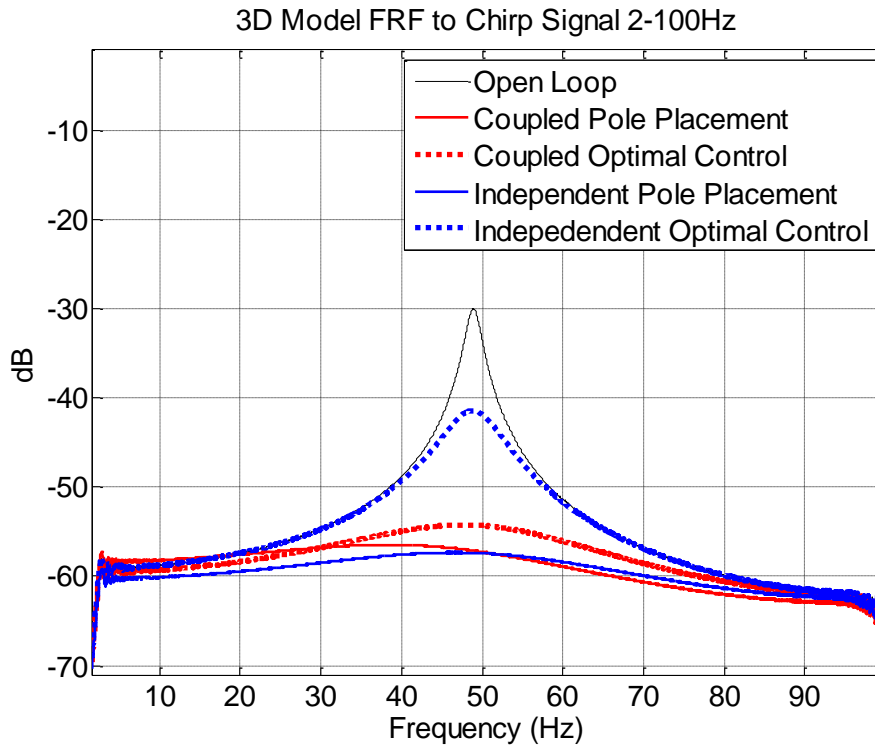
Figure 5-16 Complex Structure response to Chirp Signal from 2 Hz to 100 Hz. Sensor Y axis, Actuator Z axis, Not Co-placed

5.3.2.2 First and Second Mode Control

To control the second mode, in addition to a sensor at Y or Z axis, another sensor for X axis is necessary. Similarly another actuator is necessary to control the vibrations in X axis. Then with two actuators and two sensors the complex structure will be controlled.

i) Co-placed actuator and sensor pair will be put at 235th node at X and Y axis. A disturbance will be given from the 130th node at X,Y,Z directions. The result of two sensors are shown in Figure 5.17 and 5.18

Sensor Location - Axis	Actuator Location - Axis	Disturbance Location - Axis
235th node X axis	235th node X axis	130th node X axis
235th node Y axis	235th node Y axis	130th node Y axis
-	-	130th node Z axis
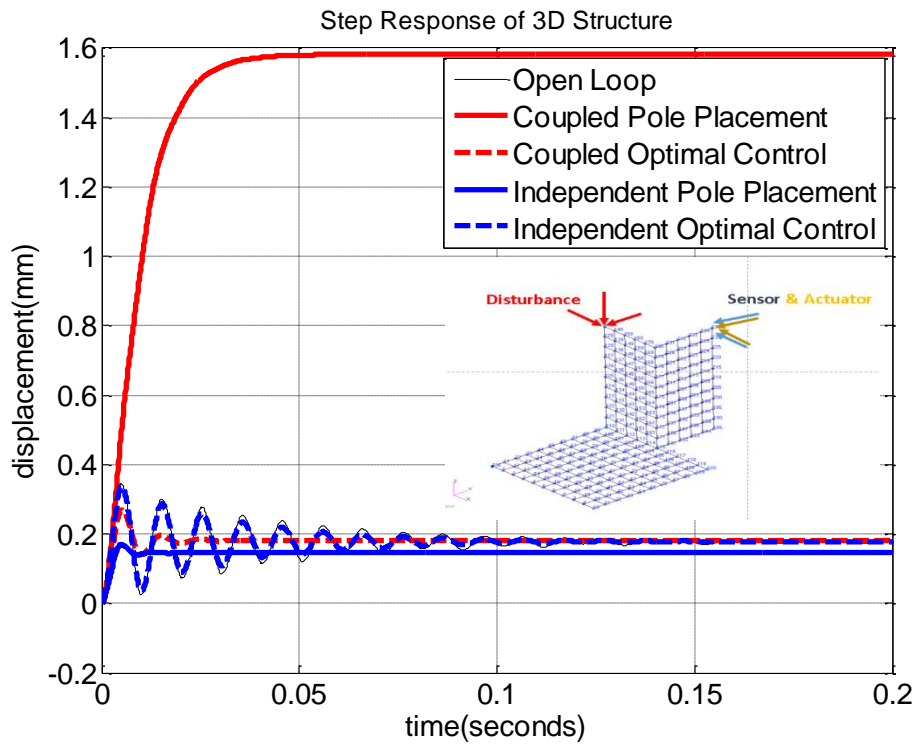
Figure 5-17 Complex Structure, response to step input X axis results.
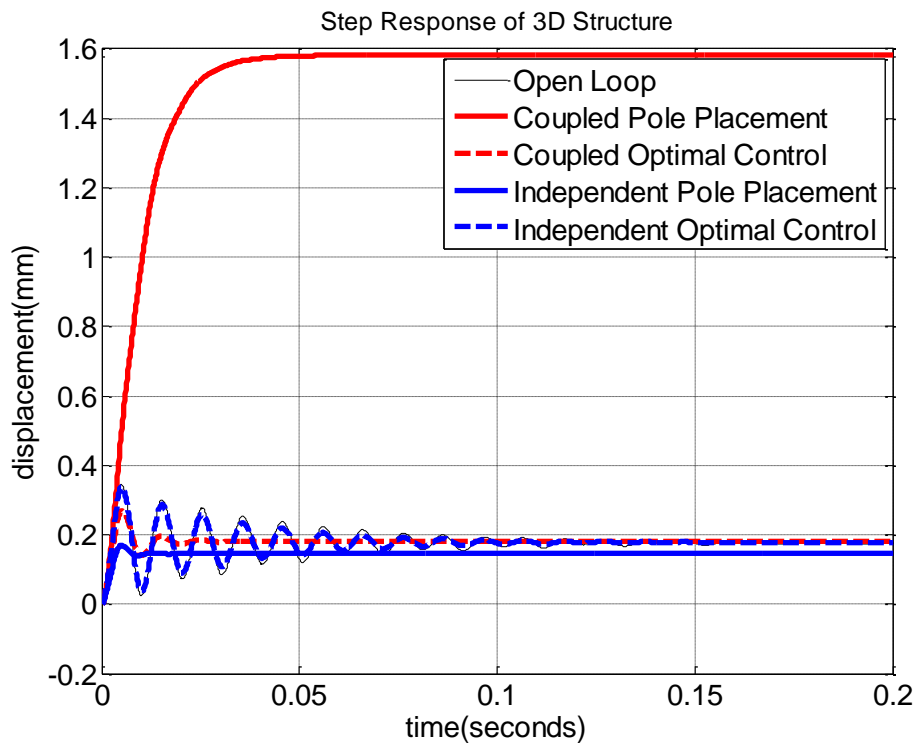
Figure 5-18 Complex Structure, response to step input Y axis results

ii) In the second case a non co-placed sensor actuator pair will be used. The results are shown in the Figure 5.19 and 5.20

Sensor Location - Axis	Actuator Location - Axis	Disturbance Location - Axis
208th node X axis	235th node X axis	130th node X axis
208th node Y axis	235th node Y axis	130th node Y axis
-	-	130th node Z axis
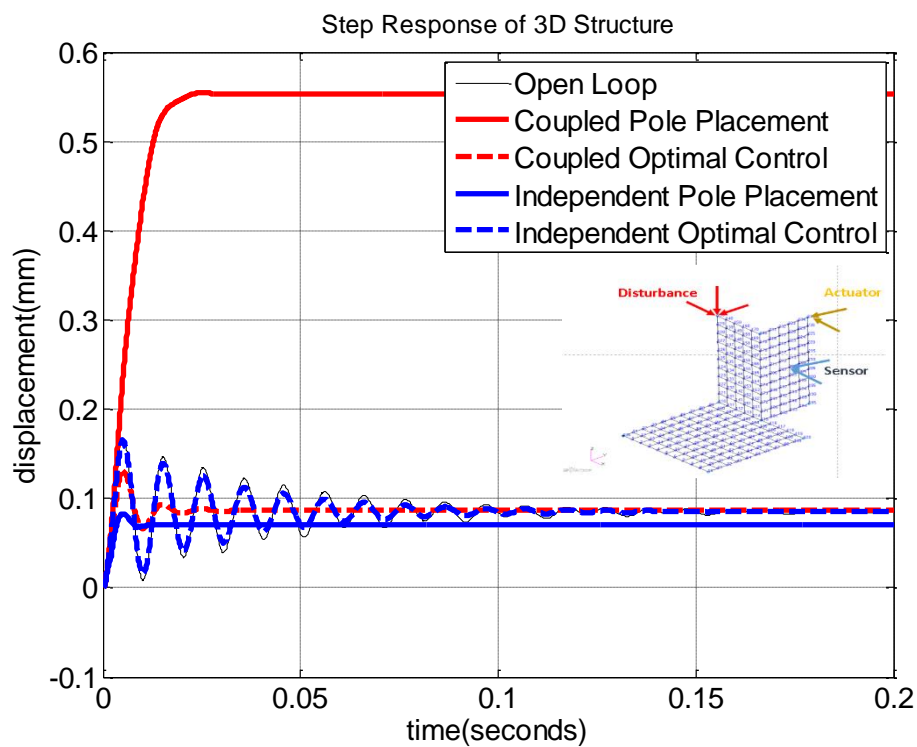
Figure 5-19 Complex Structure, response to step input X axis results. Non Co-placed sensor and actuator
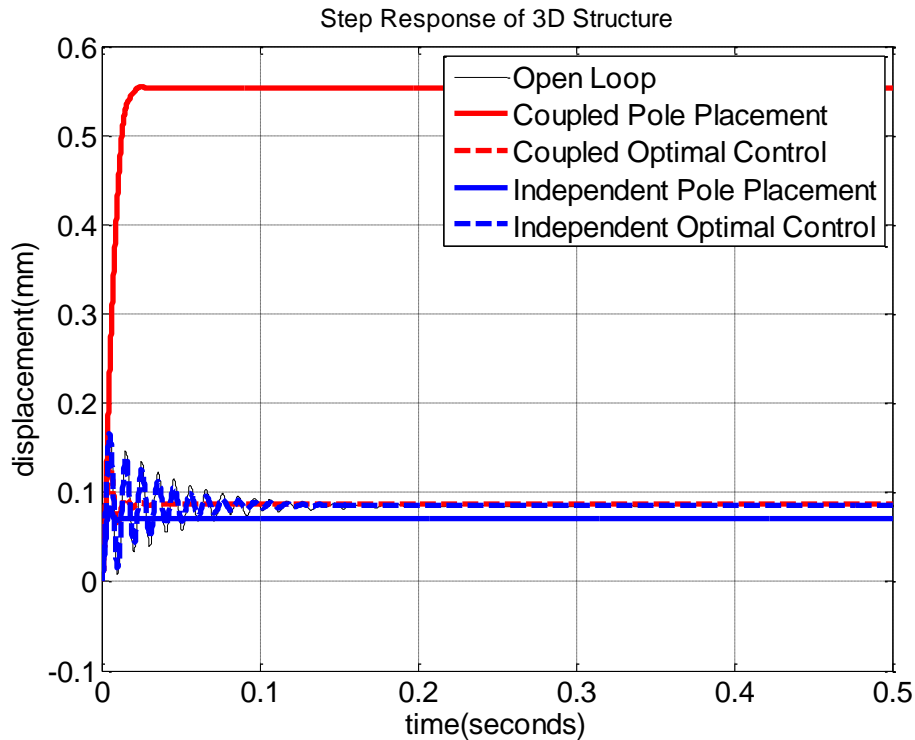
Figure 5-20 Complex Structure, response to step input Y axis results. Non Co-placed sensor and actuator

iii) In the third case frequency response function of case (ii) will be shown. Frequency between 2 Hz and 110 Hz is given in 110 seconds as chirp signal. Ode5 is used as solver with fixed time step size 1/10000. FFT is taken with the code in Appendix A. The results are shown in the Figure 5.21 and 5.22.

In the figure 5.21, it can be seen that there is a significant reduction at second resonance frequency. Coupled pole placement is not effective for lower frequencies; therefore other control algorithms are more appropriate. For this case independent pole placement offers lowest vibration levels. If one wants to optimize the actuator force optimal control schemes also offer low vibrations for lower frequencies and the resonance peak can be reduced by decreasing the R value if better performance is required. R is 0.001 at this case.
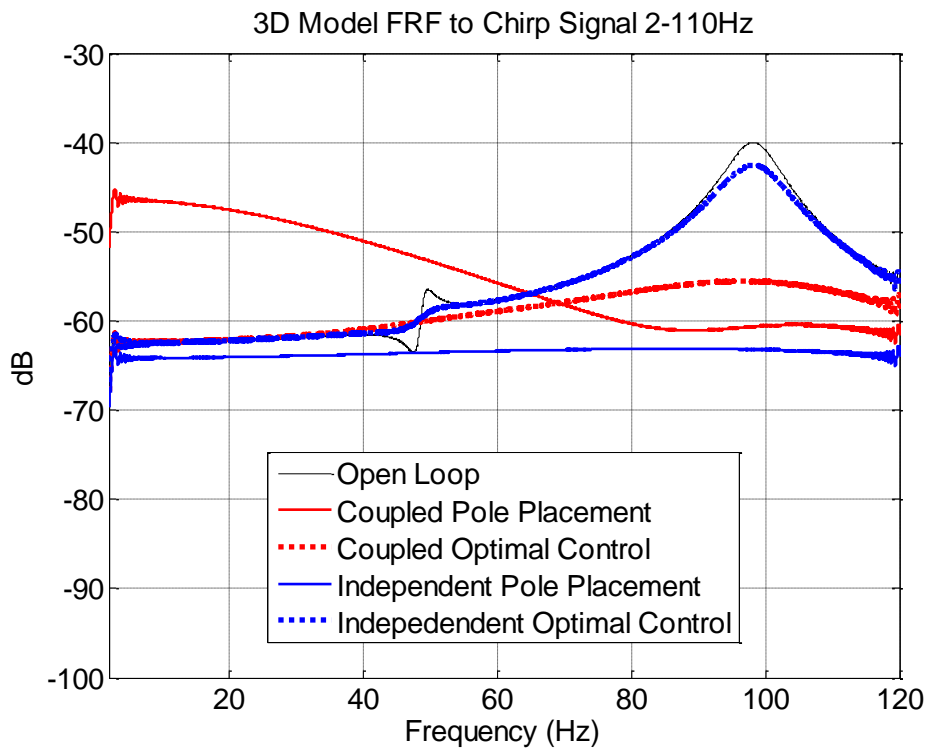
Figure 5-21 Complex Structure, X axis sensor frequency response function. Non Co-placed sensor and actuator

From figure 5.22 Y axis results can be read. First mode is dominant for Y axis and with the control algorithms the vibrations can be reduced more than 20 dB at resonance. Coupled pole placement increases the vibrations at lower frequencies, therefore other control algorithms may be chosen. However for higher frequencies coupled control is better.
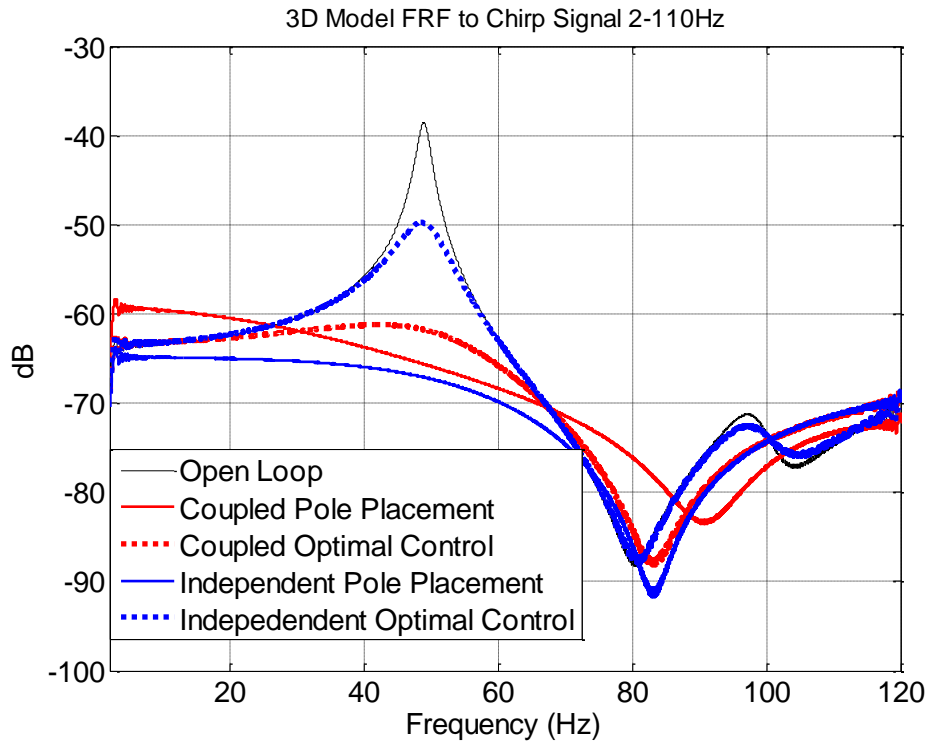
Figure 5-22 Complex Structure, Y axis sensor frequency response function. Non Co-placed sensor and actuator

5.3.2.3 *Local Mode Control (5th Mode)*

In this case study only a higher mode will be controlled assuming that it is excited by an external disturbance. Indeed its natural frequency is high(around 620 Hz) this case will demonstrate the applicability of modal space control to control local modes of a structure.

From Figure 5.11 and Table 5.5 it can be seen that node 120 is most affected by 5th mode vibrations. Then we place the disturbance to this node at Z axis. Assume that we cannot put the sensor and actuator in the same location (not co-placed) and also they cannot put on the disturbance. Actuator location is selected to be 96th node and sensor location is selected to be 108th node. Indeed they have to be located nearly as it is a local mode and it does not affect other sides of the structure.

Sensor Location - Axis	Actuator Location - Axis	Disturbance Location - Axis
108th node Z axis	96th node Z axis	120th node Z axis

The damping is tried to be located at $1/\sqrt{2}$. However coupled control cannot converge therefore the necessary damping ratio is reduced to 1/2. (i.e from 0.707 to 0.5). Then the result is shown in the Figure 5.23. For optimal control parameter R is taken as 0.0001
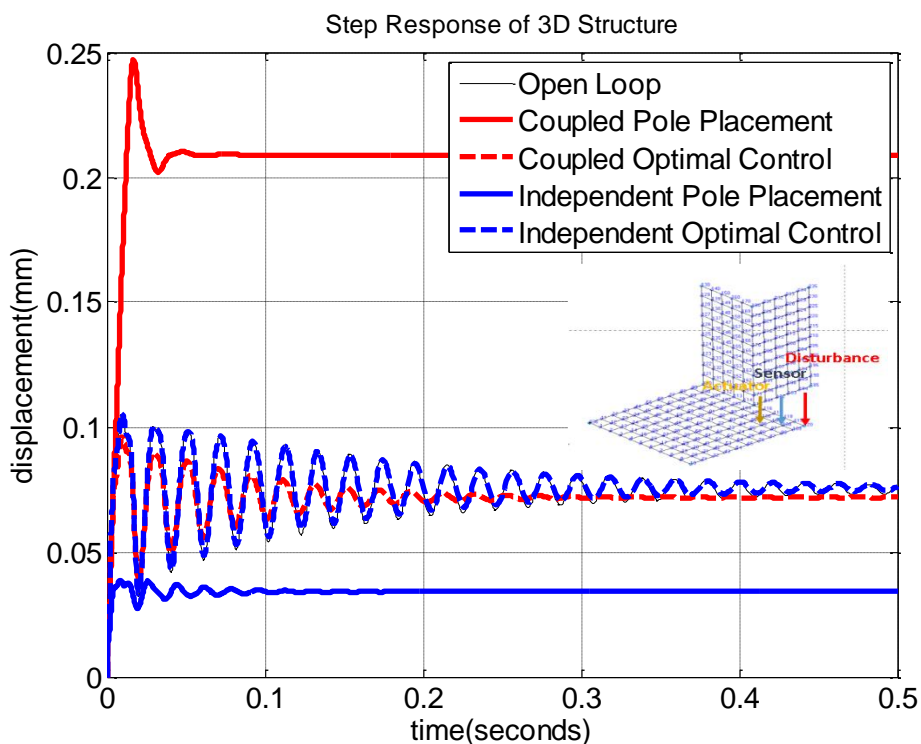
Figure 5-23 Local Mode Control Results to Step Input

An FRF analysis is done between 30 Hz and 900 Hz and results are given in the figure 5.24. It can be seen that there is a reduction around 620 Hz. Also there is reduction at 1st, 2nd and 3rd mode. But there is no reduction at 4th mode. From table 5.5 it can be seen that first three modes also has a Z direction displacement at that local area, but 4th mode does not have that displacement. Indeed it is only wanted to control the 5th mode, first three modes vibration is also reduced. This explains the good step input response of the system as it is not expected to have a good step response by only controlling 5th mode as its contribution is greatly lower than first four mode.
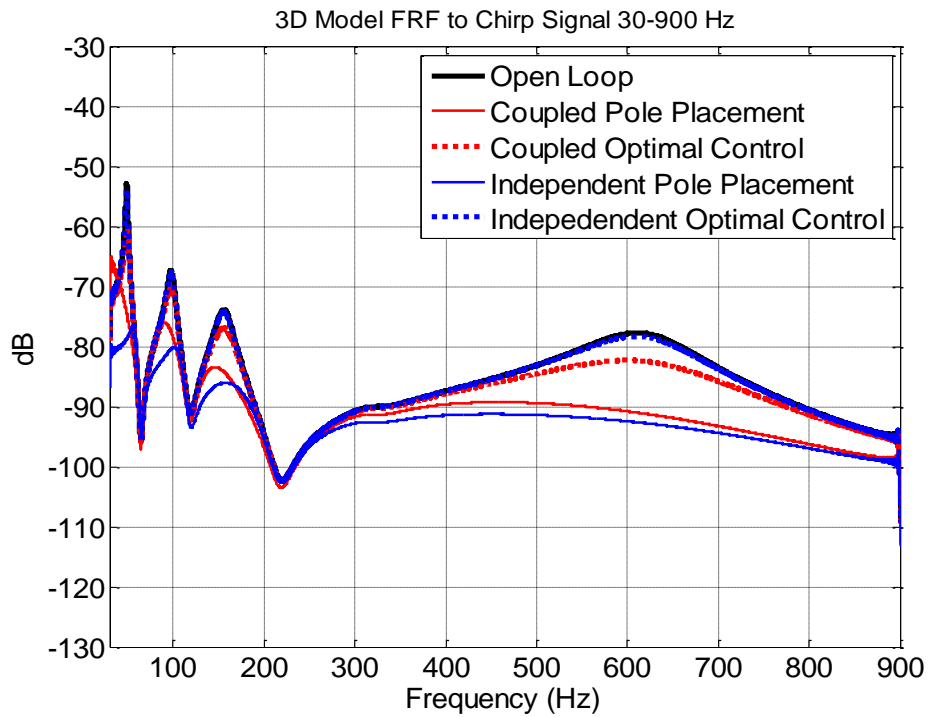
Figure 5-24 Frequency Response Function of Local Mode Control to A Chirp Excitation
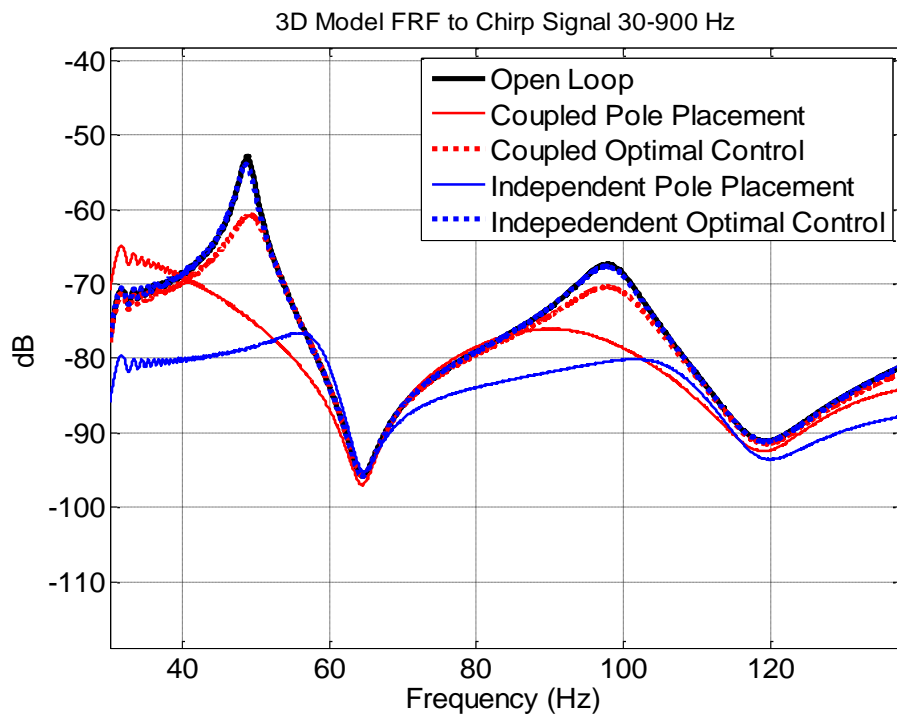
Figure 5-25 Frequency Response Function of Local Mode Control to A Chirp Excitation Close Up View First and Second Mode
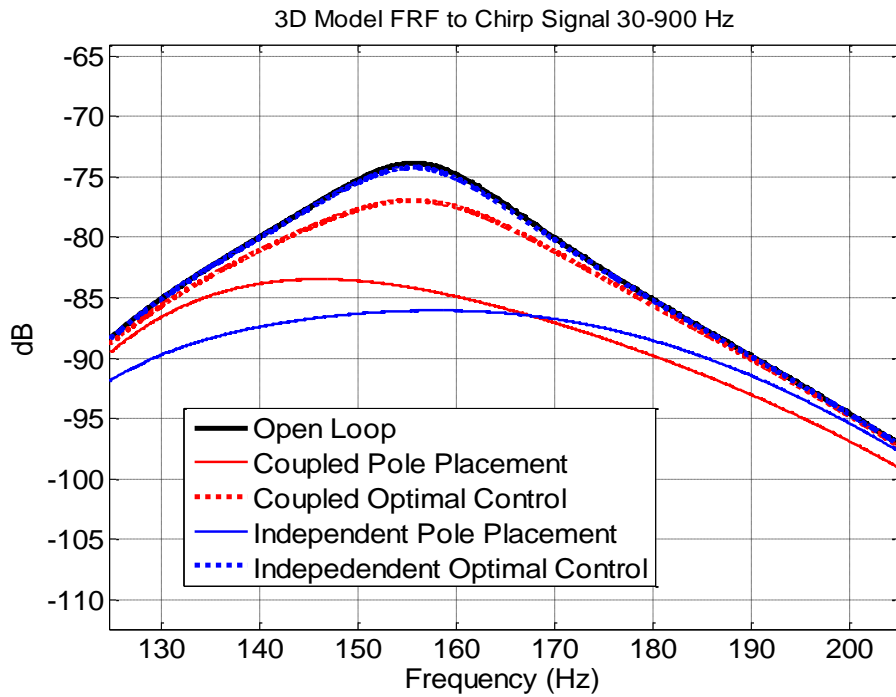
Figure 5-26 Frequency Response Function of Local Mode Control to A Chirp Excitation Close Up View Third Mode
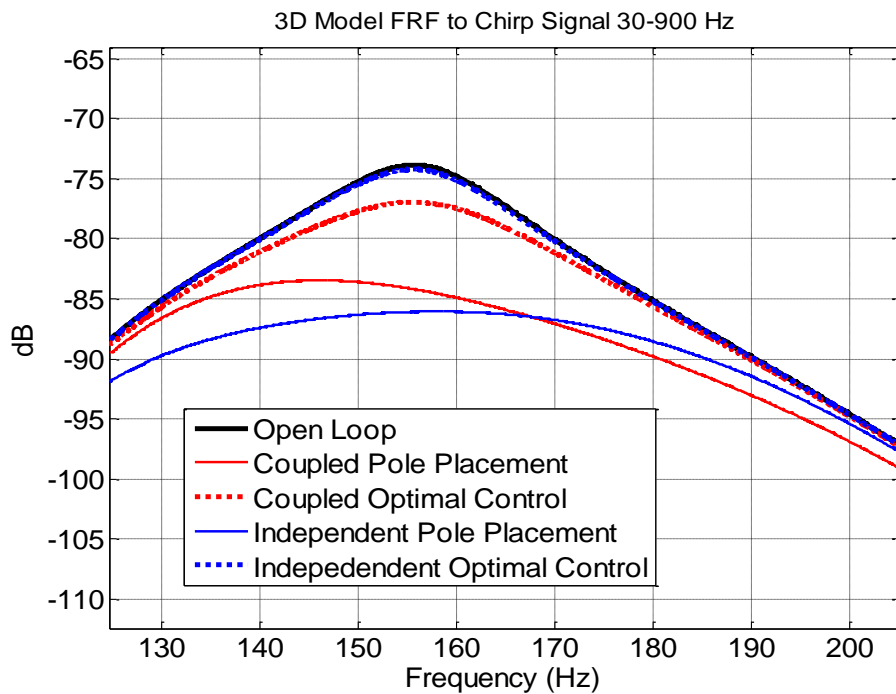
Figure 5-27 Frequency Response Function of Local Mode Control to A Chirp Excitation Close Up View Fifth Mode

CHAPTER 6

CONCLUSION

6.1   Discussion

Modal space feedback control is effective at reducing vibrations at resonances. However at other than resonance frequencies, vibrations may be amplified. By selecting proper controller this problem can be solved. If the structure is excited with forced vibrations at frequencies other than resonance frequencies one can also implement feed forward controller to improve the efficiency.

In this study displacement sensors are used to observe the system. Velocity sensors are similar to displacement sensors. However when an accelerometer sensor is introduced, D matrix is no longer a null matrix. Then observation spillover can destabilize the system easier. To prevent this problem one should use more sensors until stability is achieved.

To get the maximum efficiency from the actuator one should place the actuator(s) at the point that the mode shape value of the controlled mode(s) is(are) maximum. To reduce the control spillover, one should choose a location such that the mode shape value of uncontrolled modes are minimum. Same approach should be used for sensor placement. It will reduce observation spillover and provide better observer performance.

A proposed experimental setup can be composed of a simply supported beam/cantilever beam, accelerometer sensors and force generator(s). Force generator can be an electric motor with unbalance mass. The phase and speed of the unbalance mass must be controllable. To prevent vibrations in other directions then controlled direction, one can use a 2nd actuator that counter balances the 1st actuator. Finite element modal can be modelled with lumped masses of sensors and actuators. Also one can make an impact test to obtain FRF between actuator(s) and sensor(s). To disturb the structure a hammer can be used

for impulse input. For sinusoidal excitation a shaker table or directly a shaker can be used. Moreover an extra motor pair can be added to disturb the structure.

6.2   Conclusion

Literature review on active vibration control focused on modal domain reveals that most of the studies are limited to simple structures such as beams and plates. Therefore, it is aimed to study the application of modal domain control on more complex arbitrary shaped structures with the help of finite element analysis tools. The methodology is developed first considering vibrations of a one dimensional structure (simply supported beam) which is modelled as distributed model with partial differential equations. Then, the orthogonality property is shown and stated that each mode is independent from each other. It is also shown that the displacement, velocity or acceleration of a structure can be written as infinite sum of its modes. Finally, the independent equations in modal domain are written in state space form. They are simulated with Simulink and the results are compared with the analytical response. The response to sinusoidal input is compared with analytical formulation and the model is verified.

Later, discretization of a one dimensional structure is demonstrated. Then, the generalization of a three dimensional model formulation is studied. Discretized one dimensional model is compared with continuous model. Both are simulated in Simulink and the results are verified. Finally, a three dimensional complex shaped structure is used to show the generalized formulation.

Control studies start with the feedback control algorithms that are implemented in state space. Four algorithms are investigated, coupled pole placement, coupled optimal control, independent pole placement and independent optimal control. Controllability and observability are investigated. Finally, an observer to estimate the states of the state space model is introduced.

Case studies are presented to show the application of modal domain control. First, simply supported beam vibrations are controlled and it is shown that different number of modes can be controlled. Second, the three dimensional complex shaped structures vibrations are controlled. Co-located and non co-located control strategies are tried. Also co-oriented and non co-oriented sensor

and actuator placements are tried. It is shown that as long as states are correctly estimated sensor and actuator does not have to be co-oriented. (i.e. sensor is sensing displacement in X axis, actuator is acting force on Y axis). Furthermore, local mode vibrations of the structure are controlled. For different cases frequency response functions are obtained to show the general performance of the control forces.

6.3   Future Work

In this study it is assumed that there is no actuator or measurement noise. Therefore, a Luenberger observer was sufficient to estimate the states. For noisy actuator and sensors a Kalman Filter can be used.

Instead of using point forces on nodes, piezoelectric actuators can be implemented into the model as they are widely used in the active vibration control applications.

Observer spillover is a significant problem that alters the stability of the system. To overcome this problem a low-pass or band-pass filter can be used to filter out the residual modes.

Optimal placement of sensor and actuators are not studied in this work. However with optimal placement, number of actuators/sensors and peak force required can be reduced and stability margin of the system can be increased.

REFERENCES

[1] Nagaraj V.T., "3rd Short Course on Helicopter Design Notes", Konkuk Univesity, 2010

[2] Chopra I., Datta A., "Helicopter Dynamics", ENAE 633 Course Book, University of Maryland, 2011

[3] Tan A.C.H., Meurers T., Veres S.M., Aglietti G., Rogers E.,"Satellite Vibration Control Using Frequency Selective Feedback", Proceedings of the 42nd IEEE Conference on Decision and Control Maui, Hawaii USA,December, 2013

[4] Irvine T., "ISS Solar Panel Vibration", www.vibrationdata.com, 2010

[5] Torbati M.M., Keane A.J., Elliott S.J., Brennan M.J., Anthony D.K., Rogers E.,"Active vibration control (AVC) of a satellite boom structure using optimally positioned stacked piezoelectric actuators", Journal of Sound and Vibration vol.292, 203-220, 2006

[6] Zhi-Le W., Bo L., Yuan Z., Hao-Su X., Cheng-Hao Z.,"Satellite Vibration on Image Quality Degradation of Remote Sensing Camera", Research on Precision Instrument and Machinery(RPIM), vol.1, issue 1., 2012

[7] Irvine T., "Vibration In Rocket Vehicles Due To Combustion Instability Revision F", www.vibrationdata.com, 2011

[8] Irvine T., "Solid Rocket Motor Pressure Oscillation Frequencies Revision A", www.vibrationdata.com, 2011

[9] L. Meirovitch (1989), Dynamics and Control of Structures, Virginia, John Wiley & Sons

[10] Balas M.J., Active Control of Flexible Systems, Journal of Optimization Theory and Applications, Vol:25 No:3, 1978

[11] Meirovitch L., Öz H., "Modal-Space Control of Large Flexible Spacecraft Possessing Ignorable Coordinates", Journal of Guidance and Control, vol.3, no. 6, Nov.-Dec.,1980

[12] Meirovitch, L., & Baruht, H., Optimal Control of Damped Flexible Gyroscopic Systems. Journal of Guidance and Control, 4(2), 157-163, 1981

[13] Vasques, C., & Rodrigues, J. D., Active vibration control of smart piezoelectric beams: Comparison of classical and optimal feedback control strategies. Computers and Structures No:84, 1402-1414, 2006

[14] - Meirovitch, L., & Baruht, H, Control of Self-Adjoint Distributed-Parameter Systems, Journal of Guidance, Vol:5 No:1, 60-66, 1981

[15] Resta F., Ripamonti F.,.Cazzulani G, Ferrari M., Independent modal control for nonlinear flexible structures:An experimental test rig, Journal of Sound and Vibration 329, 961-972, 2010

[16] Lindberg Jr. R.E., Longman R.W., "On the Number and Placement of Actuators for Independent Modal Space Control", Journal of Guidance and Control, vol.7, no.2, March-April, 1984

[17] Qiu Z., Zhang X., Wu H., Zhang H., Optimal placement and active vibration control for piezoelectric smart flexible cantilever plate, Journal of Sound and Vibration 301, 521-543, 2007

[18] Jemai B., Ichchou M.N., Jezequel L., An Assembled Plate Active Control Damping Set-Up: Optimization and Control, Journal of Vibraton and Control 225, 327-343, 1999

[19] Xu B., Jiang J. S., Integrated optimization of structure and control for piezoelectric intelligent trusses with uncertain placement of actuators and sensors, Computational Mechanics 33, 406-412 , 2004

[20] Canfield R., Meirovitch L., Integrated Structural Design and Vibration Suppression Using Independent Modal Space Control, AIAA Journal, Vol 32, No: 10, 1994

[21] Meirovitch L.,Baruh H., Oz H., A Comparison of Control Techniques for Large Flexible Systems, Journal of Guidance , Vol:6, No:4, 302-310, 1983

[22] Meirovitch L., Baruh H., "Robustness of the Independent Modal-Space Control Method", Journal of Guidance, vol.6, no.1, Jan-Feb, 1983

[23] Baz, A., Poh S., Studer P., "Modified independent modal space control method for active control of flexible systems", Proceedings of the Institution of Mechanical Engineers, Part C: Journal of Mechanical Engineering Science, vol.203, no. 2, 103-112, 1988

[24] Singh S.P., Pruthi H.S., Agarwal V.P., Efficient modal control strategies for active control of vibrations, Journal of Sound and Vibration 262, 563-575, 2003

[25] Öz, H., "Independent modal-space control and estimation with distributed piezoelectric actuators and sensors", *Proc. SPIE 2715*, Smart Structures and Materials 1996: Mathematics and Control in Smart Sturcutres, 196,1996.

[26] Fang J.Q., Li Q.S., Jeary A.P., "Modified independent modal space control of m.d.o.f. systems", Journal of Sound and Vibration, vol.261, issue 3, 421-441, 2003

[27] Lin Y.H., Yu H.C., "Active modal control of a flexible rotor", Journal of Mechanical System and Signal Processing, vol.18, 1117-1131, 2004

[28] Poh S., Baz.A, "Active Control of a Flexible Structure Using a Modal Positive Position Feedback Controller", NASA Technical Report, 1990

[29] Hurlebaus S., Stöbener U., Gaul L., "Vibration reduction of curved panels by active modal control", Journal of Computers and Structures, vol.86, 251-257, 2008

[30] Serra, M., Resta F., Ripamonti F., "Dependent Modal Space Control",Journal of Smart Materials and Structures, vol.22, no.10, 2013

[31] L. Meirovitch (2001), Fundamentals of Vibrations, Virginia, McGraw Hill

[32] Inman D.J.(2006), "Vibration with Control", Virginia USA, John Wiley & Sons

[33] R. Pathi , Pole Placement Control Design, http://nptel.ac.in/, last visited November 2014

[34] Budynas R.G & Nisbett J.K (2011), Shigley's Mechanical Engineering Design 9th Edition, USA, McGraw Hill

[35] System Dynamics - The Effect of Pole Location on Response, http://www.facstaff.bucknell.edu/mastascu/econtrolhtml/SysDyn/SysDyn2Pole Location.html, last visited November 2014

[36] Kalman R.E., A New Approach to Linear Filtering and Prediction Problems, ASME Transactions, Vol. 82 Part D pp. 35-45, Journal of Basic Engineering, 1960

[37] Luenberger D.G. , An Introduction to Observers, IEEE Transactions on Automatic Control, Vol. AC-16, No:6, December 1971

[38] Fuller C.R, Elliott S. J., Nelson P.A (1997), Active Control of Vibration, USA, Elsevier

[39] Silva L.A., Inman D.J., "On the Application of Independent Modal-Space Control to Internal Variable Based Viscoelastic Bar", Proceedings of SPIE - The International Society for Optical Engineering, vol.4753, no. I, 247-252, 2002

[40] Meirovitch L., Öz H., "Stochastic Independent Modal-Space Control of Distributed-Parameter Systems", Journal of Optimization Theory and Applications, vol.40, no.1, May , 1983

[41] Raja S., Sinha P.K., Pratahap G., Bhattacharya P., "Influence of one and two dimensional piezoelectric actuation on active vibration control of smart panels", Journal of Aerospace Science and Technology, vol.6, 209- 216, 2002

[42] Chen, T., Hu C., Huang W.H., "Vibration control of cantilevered Mindlintype plates", Journal of Sound and Vibration, vol.320, 221-234, 2009

[43] Choi H.D., Bang H.,"An adaptive control approach to the attitude control of a flexible rocket", Journal of Control Engineering Practice, vol. 8, 1003-1010, 2000

[44] De Silva C.W., "Vibration Fundamentals and Practice", CRC Press, Boca Raton, London, New York, Washington D.C., 1999

[45] Patil M., "Beam Vibrations", Aerospace and Ocean Engineering Department, Virginia Tech last visited: September 2014, www.dept.aoe.vt.edu/~mpatil/courses/BeamVibrations.pdf,

[46] "Final Project - Cantilever Beam Experiment", Mechanical Engineering Department University of Massachusetts Lowell, faculty.uml.edu

[47] "Module 10: Free Vibration of an Undampened 1D Cantilever Beam", ANSYS, University of Connecticut, 2012

[48] Whitney S., "Vibrations of Cantilever Beams: Deflection, Frequency, and Research Uses", emweb.unl.edu, 1999

[49] Bhattacharjee R., "Free Vibrations of Cantilever Beam (Continuous System)", Sakshat Virtual Labs, iitg.vlab.co.in, Last visited: September 2014

[50] Ogata K., "Modern Control Engineering", 5th Edition, 2009

[51] Premount A., "Vibration Control of Active Structures an Introduction", 3rd Edition, 2011

[52] Lüleci İ.F., "Active Vibration Control of Beam And Plates By Using Piezoelectric Patch Actuators", M.Sc. Thesis, Middle East Technical University, 2013

[53] Gençoğlu C.,"Active Vibration Control Of Beams And CylindricalStructures Using Piezoelectric Patches", M.Sc. Thesis, Middle East Technical University, 2014

[54] Ardıç H., "Design And Modeling Elastomeric Vibration Isolators Using Finite Element Method", M.Sc. Thesis, Middle East Technical University,2013

[55] Arıdoğan M.U., "Performance Evaluation Of Piezoelectric Sensor/Actuator On Investigation Of Vibration Characteristics And Active Vibration Control Of A Smart Beam", M.Sc. Thesis, Middle East Technical University, 2010

[56] Batıhan A.Ç., "Vibration Analysis Of Cracked Beams On ElasticFoundation Using Timoshenko Beam Theory", M.Sc. Thesis, Middle East Technical University, 2011

[57] Kalman R.E., The Theory of Optimal Control and the Calculus of Variations, Mathematical Optimization Technique, 1963

[58] Meirovitch, Baruh, Optimal Control of Damped Flexible Gyroscopic Systems, J.Guidance and Control, 1981

[59] Meirovitch, Öz, Optimal Modal-Space Control of Flexible Gyroscopic Systems, J. Guidance and Control, 1980

[60] Messner, B., Tilbury, D., Hill, R., Taylor, J. D., Control Tutorials for MATLAB and Simulink. http://ctms.engin.umich.edu/CTMS/, 2012, last visited 2014

APPENDIX A

MATLAB CODE FOR FAST FOURIER TRANSFORM

Fast fourier transform is a method which converts time domain signals to frequency domain. Therefore harmonic signals can be visualized better. The Matlab code is given below.

```
%% Fast Fourier Transform
% code source is taken from
% http://www.mathworks.com/help/matlab/ref/fft.html
% and edited by Kemal Mersin.
%%
Sensor = 1; %Selected output sensor
s = OL.signals.values(:,Sensor)*1000; % Get the output from Simulink simout
block named OL(i.e. Open Loop), convert from meters to milimeters
L = length(s); % Get the length of the data
Fs = 10000; % Sampling Frequency


NFFT = 2^nextpow2(L); % Next power of 2 from length of y
Acc = fft(s,NFFT)/L;  % Fast Fourier Transformation of the signal
ff1 = Fs/2*linspace(0,1,NFFT/2+1);
figure, % Create a new figure
% Change to dB and plot it
plot(ff1,20*log10(2*abs(Acc(1:NFFT/2+1)))),'ko','LineWidth',1);
grid on;
hold on; % For other plots hold it on
axis([30 900 -180 -20]); % Define the axis properly
xlabel('Frequency (Hz)'); % Define the xlabel
ylabel('dB');           % Define the ylabel
```